

RETURNING MATERIALS:
Place in book drop to remove this checkout from your record. FINES will be charged if book is returned after the date stamped below.

THE DEVELOPMENT AND CHARACTERIZATION OF A FLASH-KINETIC ABSORPTION SPECTROMETER

bу

Dwight Henry Lillie

A THESIS

Submitted to
Michigan State University
in partial fulfillment of the requirements
for the degree of

MASTER OF SCIENCE

DEPARTMENT OF CHEMISTRY

ABSTRACT

THE DEVELOPMENT AND CHARACTERIZATION OF A FLASH-KINETIC ABSORPTION SPECTROMETER

Вy

Dwight Henry Lillie

A computer-based modular optical kinetic spectrometer has been developed for the purpose of studying some of the primary reactions in green plant photosynthesis. This spectrometer has the capability of detecting optical absorption changes on the order of 10^{-4} , and can follow reactions with a time constant of 2Mhz. The modularity of the system allows for differing experimental setup requirements.

A series of experiments have been performed to ascertain the spectrometer's current capabilities and limits. These involved, among others, the induced photochemistry from the probe source, electrochromic response seen in chloroplasts, proton release as measured by an indicator dye, Neutral Red. Results indicate the kinetic spectrometer reproduces the same as in the literature.

We now have the capability to probe optically the oxidizing size of PSII; both at Z the primary donor to P_{680} and at the Oxygen Evolving Complex.

to Carolynn, Curtis, and my parents

ACKNOWLEDGEMENTS

I would like to thank Dr. Gerald T. Babcock for the independence and assistance he offered throughout this project. I am grateful for the patience and time Ron Haas, Tom Clarke, and Marty Rabb spent teaching and helping me with the electronics. I am grateful to Dr. Tom Atkinson for the help in programming and de-bugging.

Finally, I thank my wife, Carolynn, for her patience and love.

TABLE OF CONTENTS

Cha	pter			Page
	r of fi			vi
ABB	REVIATI	ONS		x
1.	INTRODUCTION			1
-	1.0	PREFACE		1
	1.1	PHOTOSY	2	
	1.2	OPTICAL	20	
	1.3	· · · · · · · · · · · · · · · · · · ·		
		1.3.1	Optical	23 24
		1.3.2	Detection	25
2.	INSTRUMENT DESIGN			30
	2.0	SUBSYSTI	ens	30
	2.1	OPTICAL		30
	2.2			41
		2.2.1	Detector Amplifiers	41
		2.2.2	Timing Circuitry	48
	2.3	COMPUTE	l	53
		2.3.1	General General	53
		2.3.2	Nicolet 1074	53
		2.3.3	AIM-65 Microcomputer	55
3.	SOFTWA	SOFTWARE DESIGN		57
	3.0	PROGRAM	IING CONSIDERATIONS	57
	3.1	AIM-65		58
		3.1.1	System Execution	58
			3.1.1.1 Program Description	59
	3.2	LSI-11/02-23		61
4.	EXPERIMENTS AND FUTURE PLANS			64
	4.0	MATERIAL	S AND METHODS	64
		4.0.1	Chloroplast Preparation	64
		4.0.2	Standard Experimental Conditions	68
	4.1		EXPERIMENTS	69
		4.1.1	Steady State Effect of Probe Beam	69
		4.1.2	Flash-induced Difference Absorption	_
			Spectrum	75

Chapter			Page
	4.1.3	Effect of DCMU on the 518nm Change	77
	4.1.4	Neutral Red Absorbance Changes	80
4.2	PLANNED	EXPERIMENTS	85
	4.2.1	Spectral and Kinetic Identification	
		of Z	85
APPENDIX A			87
LIST OF PE	REPENCES.		101

LIST OF FIGURES

Figure		Pag
1.1	Z-SCHEME in green plants. Display of the linear electron transport pathway as a function of the known or inferred midpoint potentials of the redox couples involved.	4
1.2	Patterns of electron and proton transport in relation to the thylakoid membrane.	6
1.3	Z-SCHEME. Depiction of known absorbance changes and the time constants associated with the components of the photosynthetic electron transport chain.	10
1.4	OXYGEN FLASH YIELD. The oxygen flash yield in isolated chloroplasts after a long dark time as a function of the number of flashes. Kok et al. (43) were able to fit a model assuming a, a fraction of centers not undergoing $S_n \longrightarrow S_{n+1}$ transition, and β , a fraction undergoing double transitions, $S_n \longrightarrow S_{n+2}$. Computer modeling predicts dark-adapted chloroplast OECs to be 75% S_1 and 25% S_0 (68).	13
1.5	Influence of an electric field on the transition energy from S_0 , ground state to S_1 , an excited state. (A) Indicates indicates the change of the transition energy as the field is turned on. (B) The absorption band shift (above) is depicted and the net result is the derivative shape (below), and is actually seen (FIGURE 4.4).	18
2.1	OPTICAL LAYOUT of the FAS. Only relative positions are shown, distances are not to scale.	31

Figure		Page
2.2	ELECTRONIC LAYOUT of the FAS. Analogue data pathways are given in solid lines, and the digital data lines are dashed. Only the electrical pathways are shown here. Note the electrical isolation of the Laser and it's trigger circuit all other electronic components of the FAS run to a common ground (not shown).	33
2.3	DC LIGHT MODIFICATION. This layout modifies the 28V AC current in to 25V DC C1 = 2400 µF; C2,C3,C4 = 10 µF; R1 = 120 ohm; R2 = 5 Kohm, variable; D1,D2 = IN4002, protection diodes; LM338 5A,25V power regulator (National Semiconductor Corp.; Santa Clara,CA).	37
2.4	600nm CUTOFF FILTER SPECTRUM. Two such filters are used to guard the PMT from laser scattering.	39
2.5	PMT CASCADE AMPLIFIER CIRCUIT. The first stage is connected to the base of the PMT by a 6cm long, heavily shielded, conductor. This is to reduce capacitance effects and pickup of Radio Frequency. The second and third stages are then housed in a separate box. Final output runs to a sample-and-hold amplifier. Adjustable gain on the thirds stage gives overall gains between 0.1 and 10,000. For a gain of 1, the adjustable time constant ranges between 3.8Mhz and 1Hz.	42
2.6	SAMPLE-and-HOLD AMPLIFIER (S/H). The other two amplifiers after the SHA-5 are LF351s (not labelled). The input line is divided with one lead going to the SHA-5 and into the first LF351's inverting input, and the second lead ties up in a voltage summing configuration going into the scond LF351's inverting input. When the SHA-5 is in the SAMPLE mode it passes the input signal completely, it's inverted and summed with the positive signal for an output signal of 0.0V. When the SHA-5 is triggered into the HOLD mode it stores the voltage on a capacitor and holds that voltage on its	45

ouput line, it is inverted, and subtracted from the

Figure Page

present signal resulting in an output signal centered around 0.0V D.C.

49

TIMING CIRCUITY. The AIM-65 is required to bring four address lines, AO - A3, and a timing line (labelled TTL), in to run the circuitry. The 74C154 is a 4 to 16 decoder and provides 16 discrete output lines (only 12 are currently utilized). The 7400 (NAND gate) and 7404 (HEX INVERTER) are used to shape each transitions on the TTL line into pulses (detailed description in text and logic involved in FIGURE 2.8). A monostable vibrator (74121) trims the pulse duration to 2.0; and the output is fed into input of each of 7402 (NAND gate). The NAND gate selected will be the one which has its input line from the decoder LO when the other input, from the monostable, goes LO it will produce an output HI pulse of the same duration as the monostable's.

TIMING SCHEMATIC. The logic involved in transforming each transition (LO -> HI or HI -> LO) on the input TTL line, A, into a final output line, F, with one pulse per transition. The output of each gate is labelled and is matched with a time trace below.

OXYGEN EVOLUTION. This depicts typical oxygen evolving rates seen with class II chloroplasts prepared as described. These rates were obtained with freshly prepared chloroplasts. Rates obtained with freeze-thawed chloroplasts (not shown) are similar. (A) Coupled oxygen evolving rate. (B) Uncoupled oxygen evolving rate.

A typical sequence of timing events (not to scale). On the top line, A, each t; indicates the beginning of a timing cycle. The cycle repeats itself at every t;. the smaller line after the t; marker indicates that the active event timing is completed, and the AIM-65 enters an idle loop until the beginning of the next cycle. Line B is an expansion of one cycle, and line C is an expansion of the active event timing portion. Example times are given below

Figure Page

(note: all times are given with respect to the previous
event) :

<u>ti</u>	me <u>duration</u>	event	
ti ti ti ti ti t1	10ms c 0-1ms d 1-20ms e 1ms f	photoshutter open S/H - 'hold' A/D - begin converting NICOLET - begin storage S/H - 'sample' photoshutter close enter idle loop	
4.3		ffect of contiuous by the probe for: (A) nd.	72
4.4	FLASH INDUCED DIFFERENCE ABSORP line represents zero absorpt marks one point.		75
4.5	difference in absorption chan normal 518 change, and trace 166 μm DCMU. The negative spik and is the PMT's response to Time constant was less	ed to emphasize the ges. Trace A is a B is the response with e(s) are at time zero,	78
4.6		of subtracting the th 40 μ <u>M</u> N.R. with in solution. Both arp negative peaks at	81

eliminates the scatter.

ABBREVIATIONS

ATP Adenosine Triphosphate

BSA Bovine Serum Albumin

BCD Binary Coded Decimal

Ch1 Chlorophy11

DEC Digital Equipment Corporation

PDP-11, LSI-11, PDP, or LSI are often used in referring

to a DEC computers

DBMIB Dibrno-3-methyl-6-isopropyl-1,4 benzoquineone

DCMU 3-(3,4 Dichlorophenyl)-1,1 dimethylurea

EDTA Ethylenediamine tetraacetic acid

ENDOR Electron-Nuclear Double Resonance

ESR Electron Spin Resonance; often called EPR for Electron

Paramagnetic Resonance

FSK Frequency Shift Keyed

HEPES N-2-Hydroxyethyl piperazine-N'-2-ethanosulfonic acid

MPU Microprosser Unit; often called CPU for Central

Processing Unit

MV Methyl Viologen

NADPH Nicotinamide adenonine dinucleotide phosphate

NR Neutral Red

OEC Oxygen Evolving Complex

PQ Plastoquinone

PSI Photosystem I

PSII Photosystem II

Q_a/Q_b quinone species ivolved in electron transport chain

between PSII and PSII

ROM Read Only Memory

RAM Random Access Memory

RSX11M Real time multi-tasking, multi-user operating

system supported by Digital Equipment Corporation. Designed to operate on their PDP-11 mini-computers.

RT-11 Real time single user operating system supported by

Digital Equipment Corporation.

σ Standard Deviation

SHN A solution of sucrose, helpes, and salt

S/H Sample and Hold Amplifier

S/N Signal-to-noise ratio

TRIS Tris(hydroxymethyl)aminomethane

Z Primary donor to P680, also thought to be origin of

Signals IIvf and IIf

CHAPTER 1

INTRODUCTION

1.0 PREFACE

Researchers working on solar energy conversion systems would do well to pay heed to what green plants do so well. Splitting water, driving electrons "uphill" over one volt, and generally getting usable chemical energy from sunlight is not a trivial feat! Plants require the cooperation of two photons of differing energies (1.85 eV and 1.77 eV) and two serially linked light-to-energy conversion systems to produce useful energy. In the process, through their highly structured conversion system, natural photosynthetic systems can boast of the highest sustained electron transfer rates ever measured, and theoretical studies by Ross et al. (17) indicate that the maximum efficiency is 70%. As 60 to 70% of the energy of the incident photons is used for driving a charge separation across a membrane; total yield for natural photosynthetic systems approach 90% of the theoretical upper limit!

1.1 PHOTOSYNTHESIS, AN OVERVIEW

The general net reaction of photosynthesis can be written as:

$$CO_2 + H_2A \longrightarrow (CH_2O) + O_2, \qquad (1.1)$$

where H_2A is an oxidizable substance such as H_2 , H_2O , H_2S , simple alcohols, or fatty acids (in the latter two cases H_2A is also often the source of carbon for the reaction); CH_2O is stored as an energy supply by the biological system. The specific form of Equation 1.1 for green plants is:

$$6CO_2 + 6H_2O \longrightarrow C_6H_{12}O_6 + 6O_2.$$
 (1.2)

In higher plants these reactions occur in subcellular organelles known as chloroplasts, which are 10-50 micrometers (µm) in diameter, and consist of an inner and an outer membrane. The inner membrane is continuous and typically forms flattened vesicles (0.5 µm in diameter) which stack upon each other in configurations known as grana, and the outer membrane is typically sheared during preparation of class II chloroplasts. The grana are interconnected by unstacked membranes known as the stroma lamella. "Thylakoid" is the term for the individual vesicles in the grana; conventionally, the terms: class II chloroplasts, thylakoids, and chloroplasts are used interchangeably.

Equation (1.2) can be misleading in its simplicity and lack of mechanistic information as there are two distinct sets of chemical reactions which occur in photosynthesis. Light reactions, catalyzed by light, perform the actual conversion to chemical energy in the form of nicotinamide adenine dinucleotide phosphate (NADPH) and adenosine

triphosphate (ATP). The molecular structures responsible for the light reactions are located in and span the width of the thylakoid membrane. Dark reactions, otherwise known as the Calvin cycle (12), use the products of the light reactions in the reduction of CO₂ to carbohydrate, and are located in the stroma lamella. For a general introduction see reference (16).

The current nomenclature and representation of the structures involved in the light reactions are depicted in Figure 1.1, categorized by the midpoint potentials of the redox couples. Known as the Z-scheme, based on a model propsed in 1960 by Hill and Bendall (13), it has been elaborated since by Hind (14) and Avron (15), and generally accepted as an accurate model for electron flow from $2H_2O/O_2+4H^+$ to NADP/NADPH. Two photosystems, photosystem I (PSI) and photosystem II (PSII), have been shown to be linked in series (27) so that under physiological conditions electron transfer is linear, proceeding from the inner thylakoid membrane to the exterior. Figure 1.2 depicts the general orientation of the Z-scheme components in the membrane. P₆₈₀ AND P₇₀₀, the primary donors or reaction centers (RC) of PSII and PSI respectively, undergo excitation and photooxidation upon exciton transfer mechanisms into them by the chlorophyll light-harvesting systems (for a review, see 28,29). P_{680} and P_{700} undergo absorbance bleachings around 680 nm and 700 nm, Until recently both P₆₈₀ and P₇₀₀ were thought to be respectively. chlorophyll dimers (30,31) because of similarities in electron spin resonance (ESR) and electron-nuclear double resonance (ENDOR) spectra of the in vivo reaction centers and dimer chlorophyll-water adducts. Reevaluation of the data, new evidence (32,33), and consideration given

FIGURE 1.1

Z-SCHEME in green plants. Display of the linear electron transport pathway as a function of the known or inferred midpoint potentials of the redox couples involved.

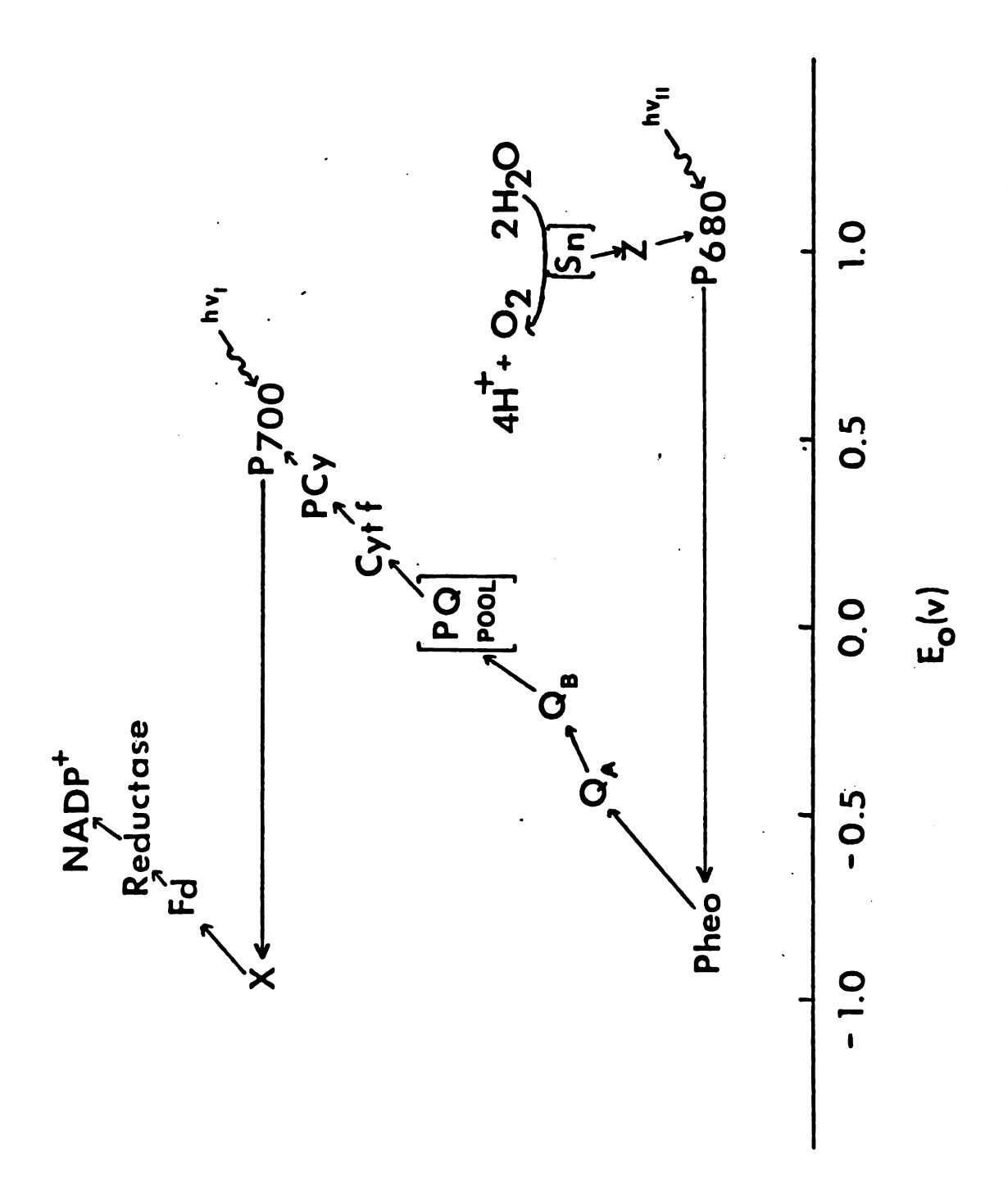
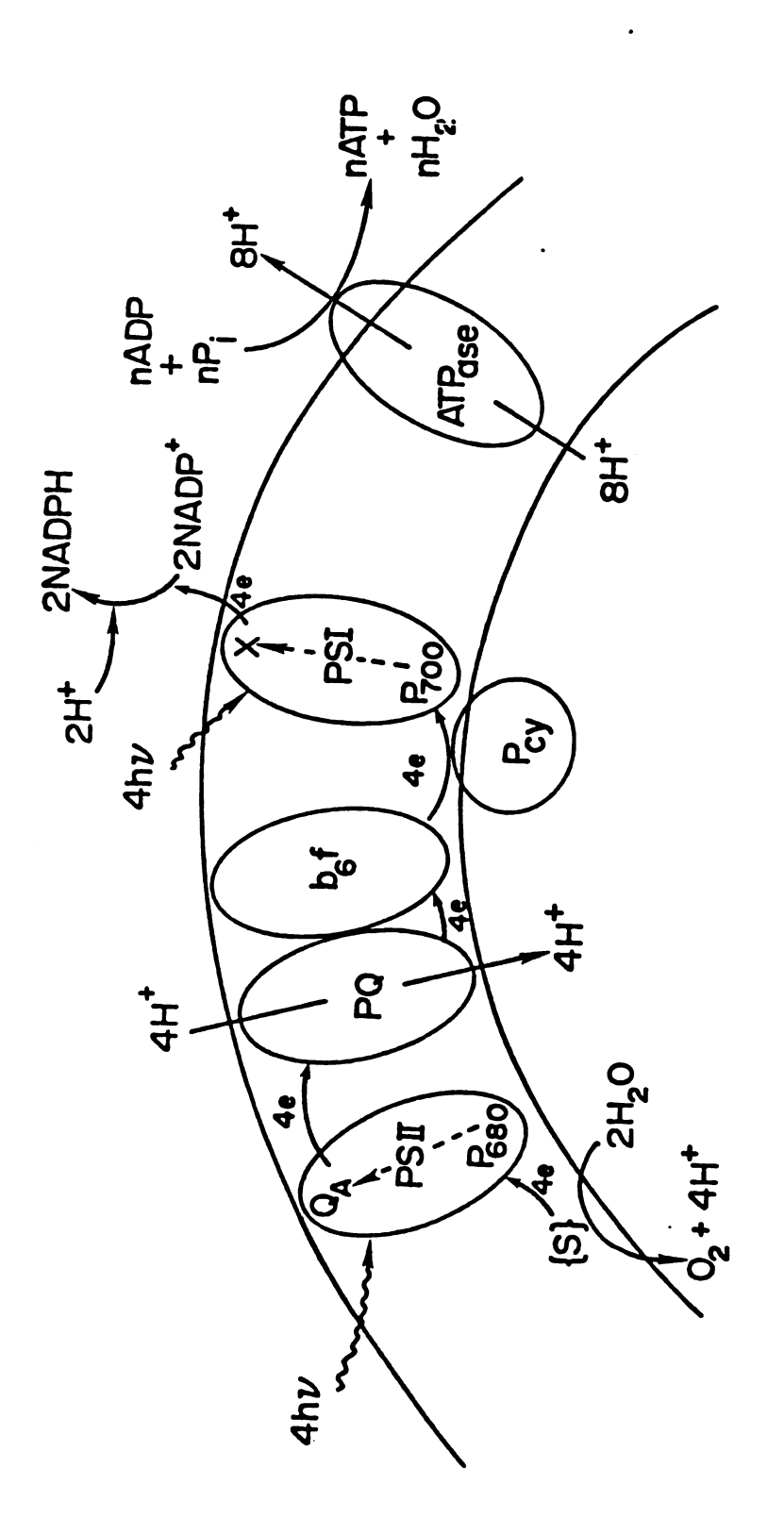


FIGURE 1.2

Patterns of electron and proton transport in relation to the thylakoid membrane.



to the protein-chlorophyll interactions, suggest that P_{680} and P_{700} could be monomers.

The primary events of photochemistry in PSII are described below. The first step involves photoexcitation of P_{680} :

$$ZP_{680}PheoQ_AQ_B \longrightarrow ZP_{680}^{\bullet}PheoQ_AQ_B,$$
 (1.3)

where Z is the donor to P_{680} ; Pheo is a pheophytin, the primary acceptor of P_{680} ; Q_A and Q_B are both plastoquinones (PQ). Initial electron transfer occurs after the photo-excitation:

$$ZP_{680}^{\bullet}PheoQ_{A}Q_{B} \longrightarrow ZP_{680}^{\dagger}Pheo^{-}Q_{A}Q_{B}.$$
 (1.4)

P₆₈₀⁺ can be detected optically at 820nm (38) and the oxidation of Pheois thought to be detectable by ESR (39). Continued electron transfer separates the charge further across the membrane (see Figure 1.2):

$$ZP_{680}^{\dagger}Pheo^{\dagger}Q_{A}Q_{B}^{\dagger}---> ZP_{680}^{\dagger}PheoQ_{A}^{\dagger}Q_{B}.$$
 (1.5)

The reduction time course of Pheo has not yet been resolved under physiological conditions. A similar reaction in the photosynthetic bacterium Chromatium has been measured and establishes an upper electron transfer rate of 10 picoseconds (ps), the fastest reaction yet measured. The reduction of $\mathbf{Q}_{\mathbf{A}}$ is accomplished in under 200 ps (40), and becomes detectable at 320nm (37) as a positive absorption change, and has been often referred to as X320 in the literature. $\mathbf{Q}_{\mathbf{A}}^{-}$ in turn reduces $\mathbf{Q}_{\mathbf{B}}$ with a $\mathbf{t}_{1/2}$ of 200-600 μ s:

$$ZP_{680}^{+}PheoQ_A^{-}Q_B^{-} \longrightarrow ZP_{680}^{+}PheoQ_A^{-}Q_B^{-}.$$
 (1.6)

 $\mathbf{Q_B}$ will accept two electrons before exchanging with a "pool" of 7-10 other PQs in the membrane. After the PQ pool a series of other carriers finally reduce $\mathbf{P_{700}}^+$. Subsequent oxidation of $\mathbf{Q_A}^-$ is between 200-400 and 600-800 μs (Recall that $\mathbf{Q_B}$ is a two electron acceptor. Upon accepting the second electron, it leaves its site and another PQ must diffuse in before additional electron transfer can occur.). $\mathbf{P_{680}}^+$ is reduced by Z (41) (also referred to as D(39)) which is in turn reduced by the oxygen evolving complex (OEC) and represented as $\mathbf{S_n}$ in reactions (1.7) and (1.8):

$$S_n ZP_{680}^{+} Pheo \longrightarrow S_n Z^{+} P_{680} Pheo,$$
 (1.7)

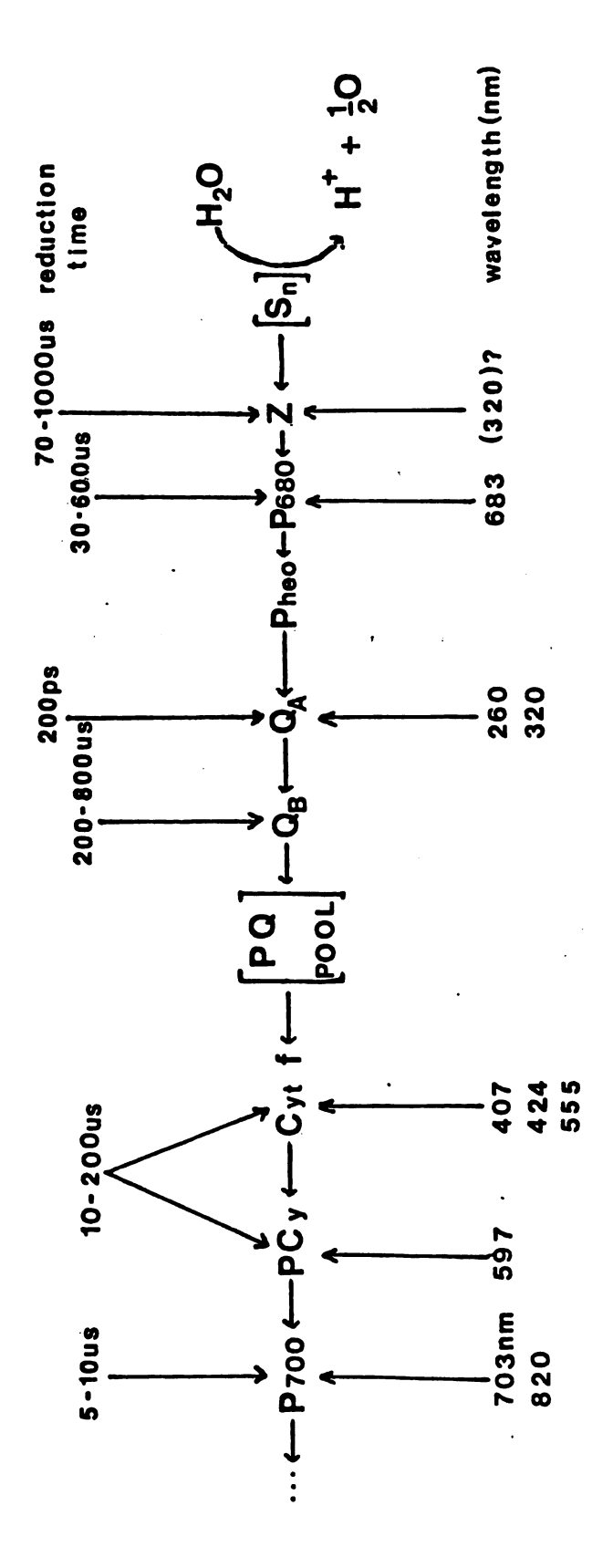
$$S_n Z^+ P_{680} Pheo \longrightarrow S_{n+1} Z P_{680} Pheo.$$
 (1.8)

Reduction times of P₆₈₀ are dependent upon sample preparation, handling, and the type of experiment performed. Single flash experiments upon dark-adapted chloroplasts by Van Best and Mathis (18) yield the fast reduction times of 30 ns. Steady state flash experiments (21) report a much slower time for reduction of 600 ns. Figure 1.3 provides an overview of the Z-scheme as a function of the time scales involved and the optically detectable components.

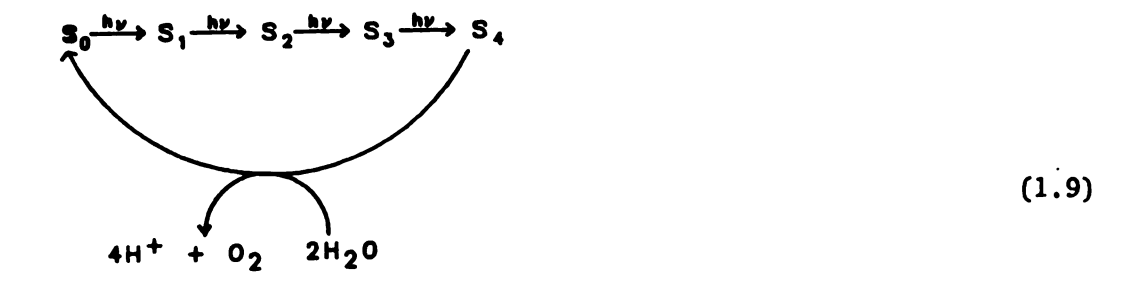
Oxidation of Z occurs during the reduction of P_{680}^{+} and its reduction proceeding at a rate determined by the redox state of the OEC. The OEC is an enzyme system probably containing four active or participating manganese atoms thought to be responsible for the oxidation of water. Under flashing light Joliet et al. (42) observed

FIGURE 1.3

Z-SCHEME. Depiction of known absorbance changes and the time constants associated with the components of the photosynthetic electron transport chain.



that the O_2 yield per flash varied with a period of four (Figure 1.4). Kok et al. (43) proposed a cyclic model for the OEC:

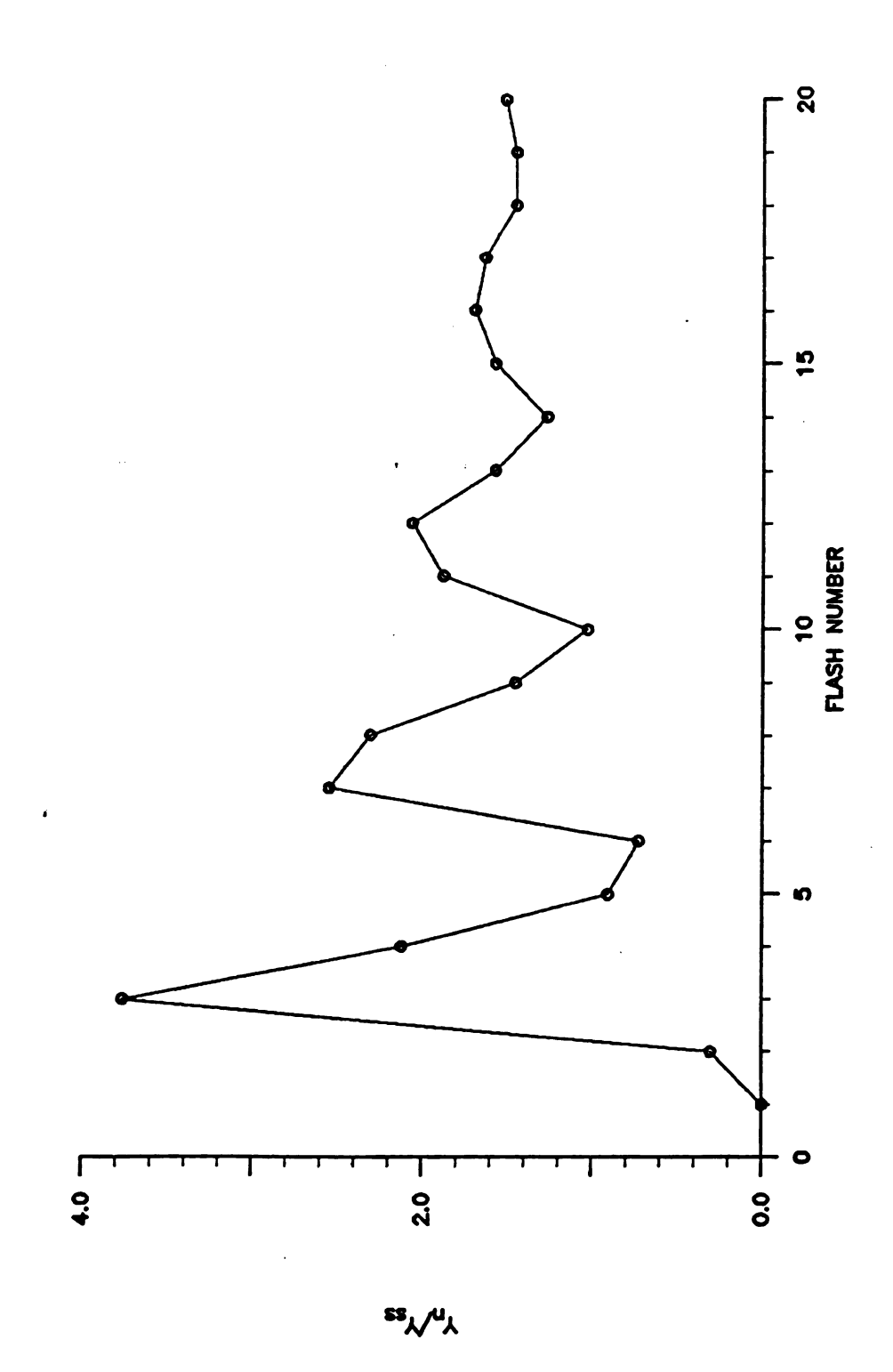


The OEC cycles through four oxidizing equivalents to oxidize two water molecules, releasing four protons to the chloroplast interior for every molecule of oxygen produced. No solid evidence is available concerning which S state transition releases protons, nor is there anything more than speculation available concerning the molecular structure of the "oxygen precursors," and their possible orientation relative to the manganese.

Extensive use of neutral red, a membrane permeant pH indicator dye, has been extensivly used by Hong and Junge (57), Theg and Junge (58), Khanna et al. (59), and Velthuys (60) to characterize proton release. Junge performed a rigorous set of control studies (61) showing that neutral red is a rapid indicator for proton release to the interior of the chloroplasts. However, wide debate continues in the literature between Fowler (46), Junge (44), Renger (45), and others concerning proton release patterns, sites in the electron transport chain where protons might be released, and involvement of manganese in water oxidation. Johnson et al. (62) have recently shown that the chloroplast

FIGURE 1.4

OXYGEN FLASH YIELD. The oxygen flash yield in isolated chloroplasts after a long dark time as a function of the number of flashes. Kok et al. (43) were able to fit a model assuming α , a fraction of centers not undergoing $S_n \longrightarrow S_{n+1}$ transition, and β , a fraction undergoing double transitions, $S_n \longrightarrow S_{n+2}$. Computer modeling predicts dark-adapted chloroplast OECs to be 75% S_1 and 25% S_0 (68).



membrane might be a proton "sink," being able to release at least 1 H⁺ per 10 chlorophyll. It is conceivable that a parallel phenomena exists in hemoglobin, namely the Bohr effect (47), in which the binding and release of oxygen changes the pK of ionizable groups in the protein causing them to release or take up protons accordingly.

Z itself has been directly detected only recently. ESR transients, signals $II_{\rm vf}$ and $II_{\rm f}$ in oxygen evolving and oxygen inhibited chloroplasts respectively, detected and characterized by Blankenship, Babcock, and Sauer (48,49,50) have been assigned to be Z·+ since 1975. The kinetics of Z should be inferable from the necessary correlation with the rapid absorption changes of P_{680}^{+} . The analysis of $II_{\rm vf}$ and $II_{\rm f}$ reveals such a correlation. Babcock et al. (41)proposed for the various oxidation states of the OEC the following scheme:

$$Z + + S_0 \longrightarrow Z + S_1 + t_{1/2} \le 100 \,\mu s;$$
 (1.10)

$$z + + s_1 \longrightarrow z + s_2 + t_{1/2} \le 100 \ \mu s^{*1};$$
 (1.11)

$$Z + + S_2 \longrightarrow Z + S_3 + t_{1/2} = 400 \, \mu s;$$
 (1.12)

$$Z + + S_3 \longrightarrow Z + S_4 + t_{1/2} = 1 \text{ ms};$$
 (1.13)

Renger and Voelker (52) have recently been able to correlate proton release transients with the extent of P^{680+} oxidation. Since then, Renger and Weiss (51) have observed an optical transient with a

^{*1)}Delayed light and electric field measurements on chloroplasts by Buttner and Babcock (unpublished) appear to indicate a $t_{1/2}$ of 70 $^{\mu}s$

periodicity of four at 320 nm under a flashing light; the phenomena appears to be related to Z. Dekker et al (76) have apparently obtained the most convincing optical evidence to date on Z·+. they report bands in the UV at 260 nm, 300 nm, and between 390 to 450nm in Tris-washed PSII preparations.

Initial photochemistry, as described reactions (1.5) and (1.6) and Figure 1.3, sets up a charge separation across the chloroplast membrane. Concurrently, large positive absorption changes have been detected between 400 - 565 nm (2), and attributed by Junge and Witt (54) to the charge separation created by the initial photochemical reactions.

The charge separation causes an electric field on the order of 10^7 V m⁻¹ and can induce absorption band shifts (electrochromism) on bulk membrane pigments such as chlorophylls and carotenoids. In general, a pigment molecule absorbing light goes from a ground to an excited state. Application of an electric field will change the transition energy between the two states if they differ in their dipole moments or polarizabilities. The frequency of the shift (for a review of theory, Liptay (55)) is related to the electric field:

$$\Delta v = -1/h(\mu^{+} - \mu^{0})\underline{E} - 1/2h(a^{+} - a^{0})\underline{E}^{2}$$
 (1.14)

where h is Planck's constant; μ^{\bullet} and μ_0 are dipole moment vectors of the excited and ground states respectively; \underline{E} is the electric field strength vector; and a^{\bullet} and a° the polarizabilities of the excited and ground states respectively. It has been observed that the change in absorbance is linear with respect to the membrane potential (see Reinwald et al. (70) and Amesz and De Grooth (71)). Carotenoids,

however, should display no such behaviour as they do not possess a dipole moment. Schmidt (72) proposed the presence of a permanent local electric field in the membrane causing an induced dipole in the carotenoids. This induced dipole would be responsible for the linear dependence of the absorbance shifts in carotenoids due to the externally applied fields. Figure 1.5a illustrates the shift in energy levels and Figure 1.5b, the shift of an absorption band induced by an electric field.

The 518 change *1) has a rise time of less than 20ns after a short laser flash and has a decay time of 10ms - 1s depending upon membrane permeability to ions and the pH gradient across the membrane. Contributing to the total electric field are two photoreaction charge separations from PSII and PSI. Selectively blocking PSI or PSII from operating decreases the maximum absorbance change by half (56).

The electron transfer chain can be altered selectively by inhibitors. The reaction in (1.5) can be blocked by 3-(3,4 dichlorophenyl)-1,1-dimethylurea (DCMU).

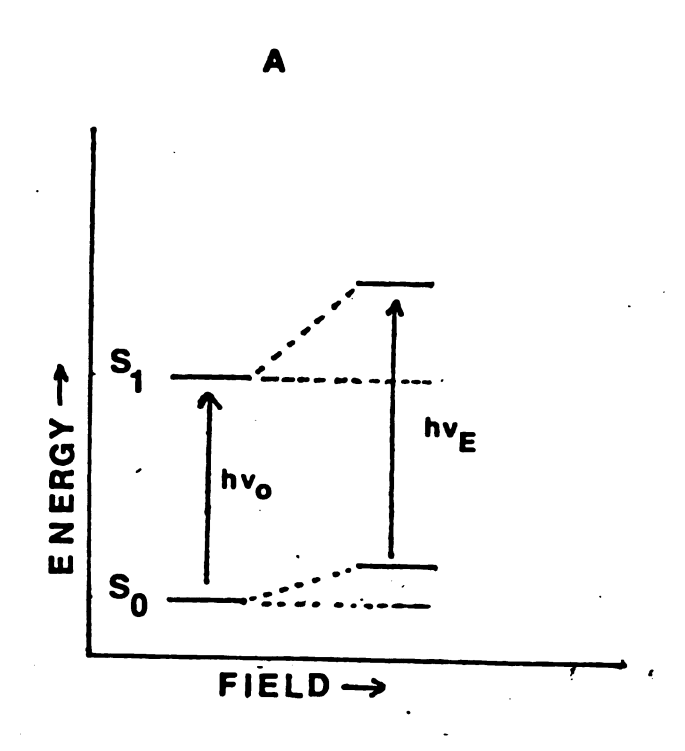
2,5-Dibromo-3-methyl-6isopropyl-1,4 benzoquinone (DBMIB) blocks
Equation (1.6) and washing with

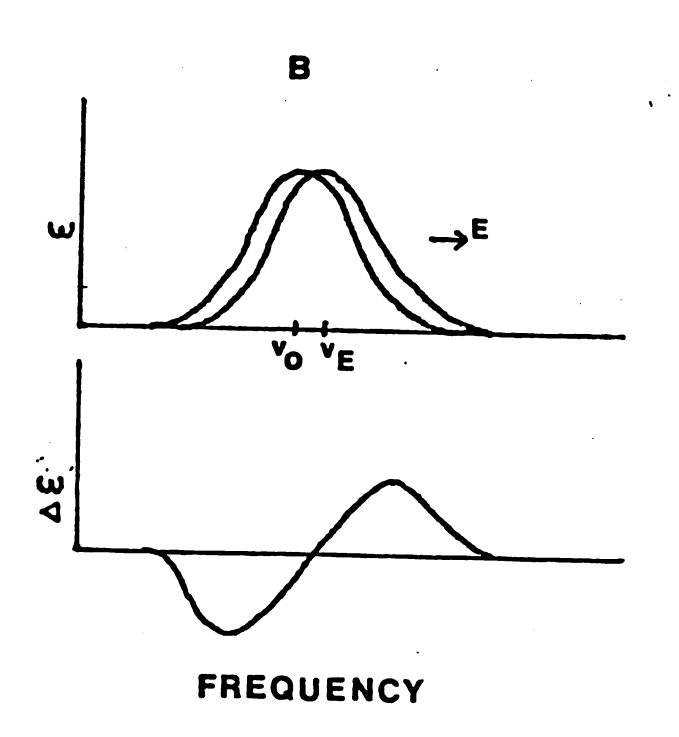
Tris(hydroxymethyl)aminomethane (TRIS) during chloroplast preparation blocks Reaction (1.8). Addition of electron donors such as benzidine or ferrocyanide, electron acceptors such as methyl viologen (MV) or ferricyanide, and a blocker for PSI or PSII allows selective probing of

^{*1)} This refers loosely to a large positive absorption band observed from 515 to 540 nm; in the literature it's referred to as the '515', the '518', or '522' change depending, of course, on the wavelength it's measured at.

FIGURE 1.5

Influence of an electric field on the transition energy from S_0 , ground state to S_1 , an excited state. (A) Indicates indicates the change of the transition energy as the field is "turned on". (B) The absorption band shift (above) is depicted; and the net result is the derivative shape (below), and is actually seen (FIGURE 4.4).





one photosystem or the other. Under altered conditions the requirements for very fast electron transfer may no longer hold true and back or cyclic electron transfer reactions can occur; see for example Hong et al. (53).

1.2 OPTICAL ABSORBANCE THEORY

For induced transitions in a molecular system, the incident photon must be of energy equal to the difference in energy between two states. The probability of the absorption of a photon in unit time of energy equal to:

$$\Delta E_{(1m|kn)} = E_{(1m)} - E_{(kn)},$$
 (1.15)

where |lm> is a lower vibronic state and |kn> a higher one, is:

$$Pia_{\langle lm|kn \rangle} = B_{\langle lm|kn \rangle} + p(\omega_{\langle lm|kn \rangle}), \qquad (1.16)$$

where $B_{\langle lm|kn\rangle}$ is the Einstein transition probability coefficient for induced absorption, and $p(\omega_{\langle lm|kn\rangle})$ the radiation density for frequency $\omega_{\langle lm|kn\rangle}$. In a similar fashion, the probability of induced emission can be expressed as :

$$Pie_{\langle kn|1m\rangle} = B_{\langle kn|1m\rangle} + p(\omega_{\langle kn|1m\rangle}), \qquad (1.17)$$

where $B_{\langle kn|1m\rangle}$ is the Einstein transition probability coefficient for induced emission and is also equal to the coefficient for induced absorption. One other transition, the probability of spontaneous emission, is expressed as:

$$Pse_{\langle kn|1m\rangle} = A_{\langle kn|1m\rangle} + p(\omega_{\langle kn|1m\rangle}), \qquad (1.18)$$

where $A_{\langle kn|1m\rangle}$ is the Einstein transition probability coefficient for spontaneous emission.

Under steady state or equilibrium conditions the probability of absorption equals the probability of emission

$$Pia = Pie + Pse. (1.19)$$

For populations of the states $|1m\rangle$ and $|kn\rangle$ of $N_{|1m\rangle}$ and $N_{|kn\rangle}$, respectively, the total probability for absorption and emission of radiation of $\omega_{\langle 1m|kn\rangle}$ is :

$$Ptot = Pie^{+}N_{|kn\rangle} + Pse^{+}N_{|kn\rangle} - Pia^{+}N_{|1m\rangle}$$
 (1.20a)

$$= A_{\langle kn|1m\rangle^{\Phi_{p}(\omega_{\langle kn|1m\rangle})} + B_{\langle kn|1m\rangle^{\Phi_{p}(\omega_{\langle kn$$

As an example, consider a system in thermal equilibrium at 298K and a photon at wavelength 600 nm ($\Delta E = 2.07 \text{eV}$). The ratio of populations is given by the Boltzman distribution law:

$$N_{|kn\rangle}/N_{|1m\rangle} = e^{-\Delta E/\underline{k}T} = 9.45 * 10^{-36},$$
 (1.21)

where <u>k</u> is the Boltzman constant and T = 298K. Therefore, the result of an incident photon in resonance with an energy state of a system is the absorption of radiation and transition to a higher (excited) state. The Einstein coefficients can be determined empirically or calculated from first principles.

For flash absorption measurements where essentially two perturbations of the system occur, the situation is little changed but conceptually harder to visualize. Recall the probability of a transition is proportional to the radiation density (and this in turn is proportional to the energy flux or actual input intensity); if a "probe" beam's intensity is kept low the ground state

 $(S^{O})^{\frac{1}{2}})^{n}$ is preferentially populated and competing processes are minimal. Any transitions would only be between ground and the first excited singlet state (S^{n}) .

An intense exciting flash — as from a laser — would cause a transition from S_0 ——> S^n (ground and the nth excited singlet respectively). She probe would continue to cause the ao ——> S_n transitions, and possibly S_n ——> S_{n+1} transitions if the resonance frequency were still the same. Assuming only the S_0 ——> S_1 transition is active, an increase in the transmitted intensity of the probe would be detected as the concentration of the molecular state responsible for the S_0 ——> S_1 transition would have been depleted.

Beer's Law provides a relation between transmitted light and the concentration of the absorbing species. The differential form:

$$-AI = a(x) + I + C + A1$$
 (1.22)

where $_AI$ is the attenuation of light intensity (for this case, it is the probe) per ΔI length, $a(\omega)$ is a proportionality constant related to the Einstein extinction coefficients, I is the initial radiant energy, and C

^{*1)}Do not confuse the use of S in referring to molecular states with the S states of the OEC discussed earlier.

the concentration of absorbing species. Integration yields :

$$I = I^{0}e^{-a(\omega)} * C * 1, (1.23)$$

OI

$$I = I^{0}10^{-8} * C * 1, (1.24)$$

where s is the decadic extinction coefficient. Rearranging yields

$$A = -\log(I/I^{\circ}) = \epsilon + C + 1, \qquad (1.25)$$

a linear relationship between absorbance and concentration.

1.3 EXPERIMENTAL APPROACHES

Norrish and Porter (1) are usually credited with having first successfully observed fast photolytic transient products of small gas molecules. Since that time flash experimental protocol has evolved considerably. Electronic detection of events lasting no more than 5 to 10 nanoseconds (ns) is practical; however, for sub-nanosecond time resolution researchers are forced to use streak cameras. The trade-off comes from a decreased sensitivity at the higher speeds as shown later. The basic "classical" setup differs little from conventional UV-VIS spectrometers in terms of the optical path and the positions of the components relative to one another. Many researchers, though, will alter the position of one or more of the components to achieve optimal response for the particular application. Junge (2) and Mathis (3) discuss in general the requirements and considerations that go into the design of fast optical detection equipment. Basically, the designs can

be divided into two sub-systems as follows: optics and detection. As our concern is principally with nano- to micro-second resolution, the discussion addresses this application with digressions where appropriate.

1.3.1 Optical -

The probe beam, monochromator or interference filter, focusing optic(s), and detector are usually mounted on a heavy optical rail. Exciting source and focusing optic(s) are placed at right angles to the sample. The heavy optical rail will minimize effects of any high frequency vibrations and insure stability of the focus. Distances between sample cell and detector are very critical.

Chloroplasts are highly scattering; incident light will be scattered into the solid angle around the collimated probe beam. As the detector is moved further from the sample it receives less and less of the scattered light and of the signal of interest. Fluorescence also emits light into the solid angle and becomes a significant portion of the signal detected if the detector is too close, thus resulting in an apparent decrease in absorbance. Modulation of the probe beam and demodulation of the output signal can be done if the interference is too great as fluorescence emission will not contain the modulated component and will be extracted from the output signal when demodulation is performed. Typical modulation techniques are on the order of 100 KHz while fluorescence lifetimes in chloroplast systems are on the order of

Photons from the exciting source itself, typically a laser, or Xeon

flashlamps, are to be excluded as the detector will respond to all incident photons. Some designs have used a second monochromator with a wide open bandpass before the detector to eliminate stray light; however, in highly scattering samples, or when the signal is small, this is usually unfeasible. Even filters between sample cell and detector designed to cut off radiation at the exciting wave length will have an attenuation of only two or three absorbance units (see Figure 2.5). Correspondingly, the transmitted intensity could still be orders of magnitude more intense than the probe beam. If the detection of this exciting light were only of the duration of the flash, which has to be very short in regards to the event under study, then the experiment may be valid. However, if the detector or amplification circuits are overloaded an apparent absorbance decrease can be detected. Valid information may still exist within the relaxation curve, but its resolution can be difficult and questionable.

1.3.2 Detection -

Primary factors in the design of electronic detection circuitry are the signal-to-noise (S/N) level, frequency response of the discrete components as well as the system as a whole, gain, stability, and the type of photodetector used.

Van Best and Mathis (4,5) utilize a silicon photodiode (UDT PIN 10, United Detector Technology; Culver City, CA) and are able to detect at least $\Delta A = 5.0 * 10^{-4}$ in photosynthetic systems between 515 and 820 nm with an optimal response between 200Hz - 1MHz. Other photosynthetic researchers, Junge (6) and Crofts (7) for example, utilize

photomultiplier tubes (PMT). Ingle and Crouch (8) have noted that, in considering the type of detector alone, except for applications where the probe is of very high intensity, the S/N level obtained with a photomultiplier tube is greater than with a photodiode. Alternatively, Bernstein, Rothberg, and Peters (9) have described a photoacoustic detection technique applied to low concentration and transients of benzophenone on a picosecond time scale. Though not applied to photosynthetic systems their results indicate sensitivity as well as high time-resolution. Other fast nanosecond and sub-nanosecond instruments use a flash probe beam in which the probe beam is pulsed for a very short time at discrete intervals after the exciting flash have been described. Though S/N enhancement is gained over more conventional continuous probe beam instruments, the time required to perform the experiment is much longer than with conventional datum has to be collected individually. as each setups photosynthetic measurements, to insure integrity of the biological system, this requires all experiments to be performed at 0°C or with repeatedly changed sample.

In most cases, the maximum frequency response of the system is determined by the amplification circuitry and not the detector. The Gain-Bandwidth Product (GBP) is a constant and determined by the design of an amplifier, and it essentially gives a measure of the highest frequency response for a particular gain. As an example, the BB3551J (Burr-Brown; Tucson, AR) has a GBP of 50MHz; a gain of 50 reduces the frequency response to 1MHz. To achieve high gain and maximal frequency response several amplifiers are often set up in series. Known as

cascade amplification, the series possesses a maximum frequency response limited by the smallest bandwidth of the individual amplifiers:

$$w_2^2 = (2^{1/n} - 1)^{1/2} * w_1 \tag{1.26}$$

where ω_2 is the high end frequency response, n is the total number of amplifiers, and ω_1 is the smallest maximum frequency response of n amplifiers.

Noise is the major limiting factor in the detection of small fast transients. Every component in an electronic circuit injects a finite quantity of noise into the signal being processed. Minimization of noise without severe signal distortion must occur in the photodetector. Amplifiers operating on a signal containing noise will process both equally. A PMT's response to light is proportional to the intensity of the light striking the surface, and can be expressed as:

$$i = \emptyset * Q * \Delta \tau, \qquad (1.27)$$

where i is the raw output signal (current); Ø the photon flux upon the photocathode surface; Q the quantum efficiency of the PMT; and AT the time interval. Photons striking the surface of the PMT are randomly distributed in time, and the PMT's output reflects this, the standard deviation being:

$$\sigma = (N_p)^{1/2} = (\emptyset Q \Delta \tau)^{1/2},$$
 (1.28)

where σ is the standard deviation; and N_p is the number of photons striking the PMT face in the time interval $\Delta \tau$. Noise from the PMT, in this context, can be defined as the root-mean-square (rms) or standard

deviation of the signal, σ . Thus Equation (1.29),

$$S/N = i/\sigma = (\emptyset Q \Delta \tau)^{1/2},$$
 (1.29)

provides an expression for evaluation of the S/N.

Improvements of S/N can be achieved by increasing the photon flux across the PMT, increasing the time interval, or using a PMT with a photocathode of a higher quantum efficiency. Equation (1.29) demonstrates why detection of fast transients is difficult, due to short time intervals the S/N is necessarily limited.

A factor not considered in this discussion is the operating temperature of the system. Electrons are released from the photocathode surface after work has been done to remove them. PMTs maintain very high potential drops of 500-1500V in order to lower the apparent work function; therefore, a significant fraction of the electrons available at the surface will possess enough energy to leave without benefit of a photon. This is known as "dark current," and can be a significant fraction of the maximum allowable current of the PMT. Additionally, the noise in the resulting signals is much higher. Water cooling of the housing of the PMT can reduce dark current noise levels an order of magnitude of more.

As a result of Equation (1.29) many researchers resort to "signal averaging" to enhance their signal to noise, and the gain to be expected can be expressed as in Equation (1.30):

$$(S/N)_{M} = M^{(1/2)} * (S/N)_{1},$$
 (1.30)

where N is the number of repetitions; $(S/N)_1$ the signal to noise ratio for one flash; and $(S/N)_M$ the signal to noise ratio for N flashes.

It quickly becomes obvious that maximal gain of signal averaging is within the first few iterations. Extremely small signals have to be elucidated in some other manner than signal averaging. In photosynthetic systems experimental times at room temperature cannot exceed 10 to 15 minutes as as irreversible damage to the electron transport chain will then have occurred.

CHAPTER 2

INSTRUMENT DESIGN

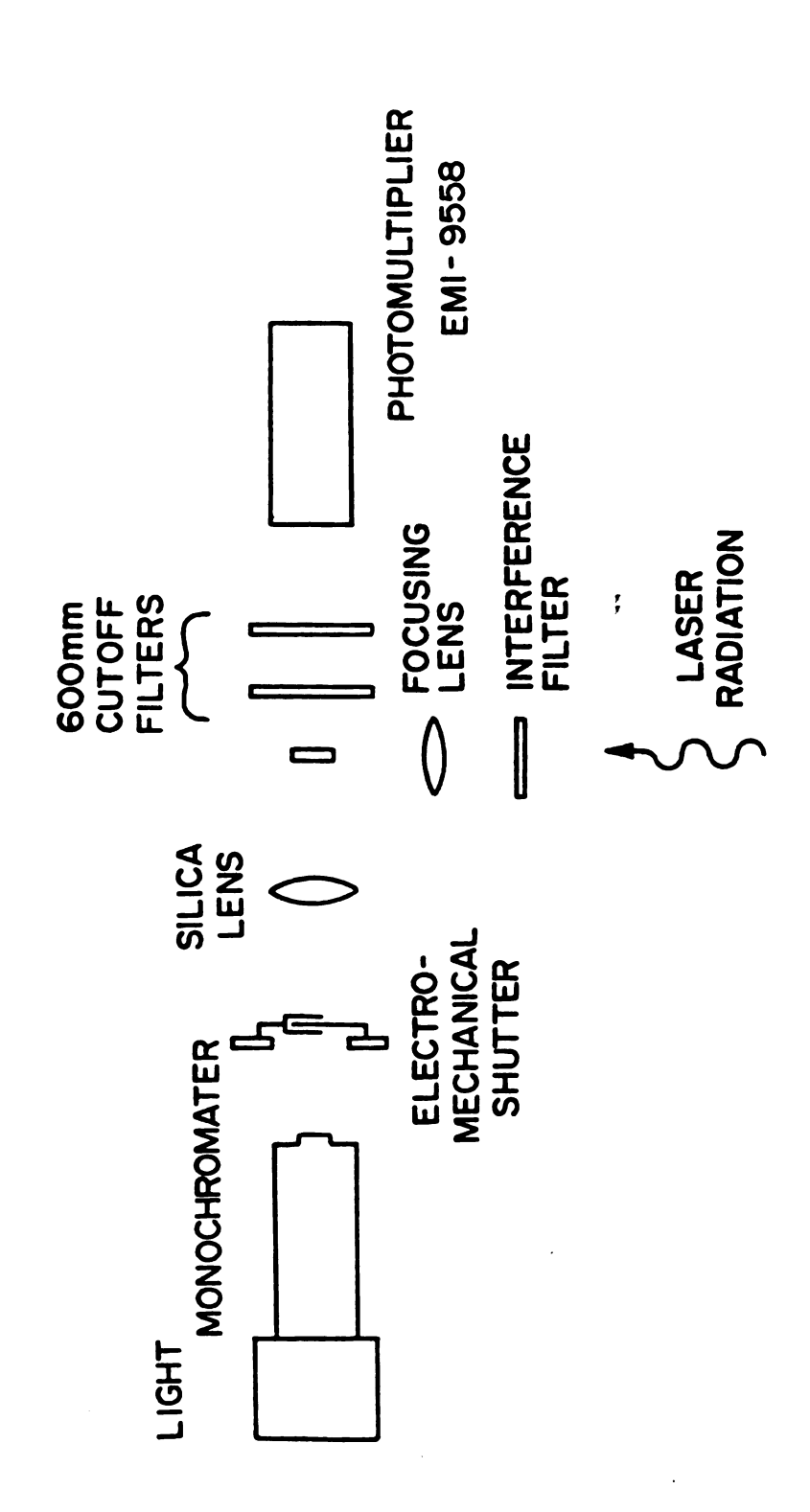
2.0 SUBSYSTEMS

The Flash Absorption Spectrometer (FAS) has three principal systems or levels involved in its design: optical, electronic, and computer. The following sections will deal with each in a sequential manner; however, considerable overlap exists between the systems. Layouts of the systems are as in Figures 2.1 and 2.2.

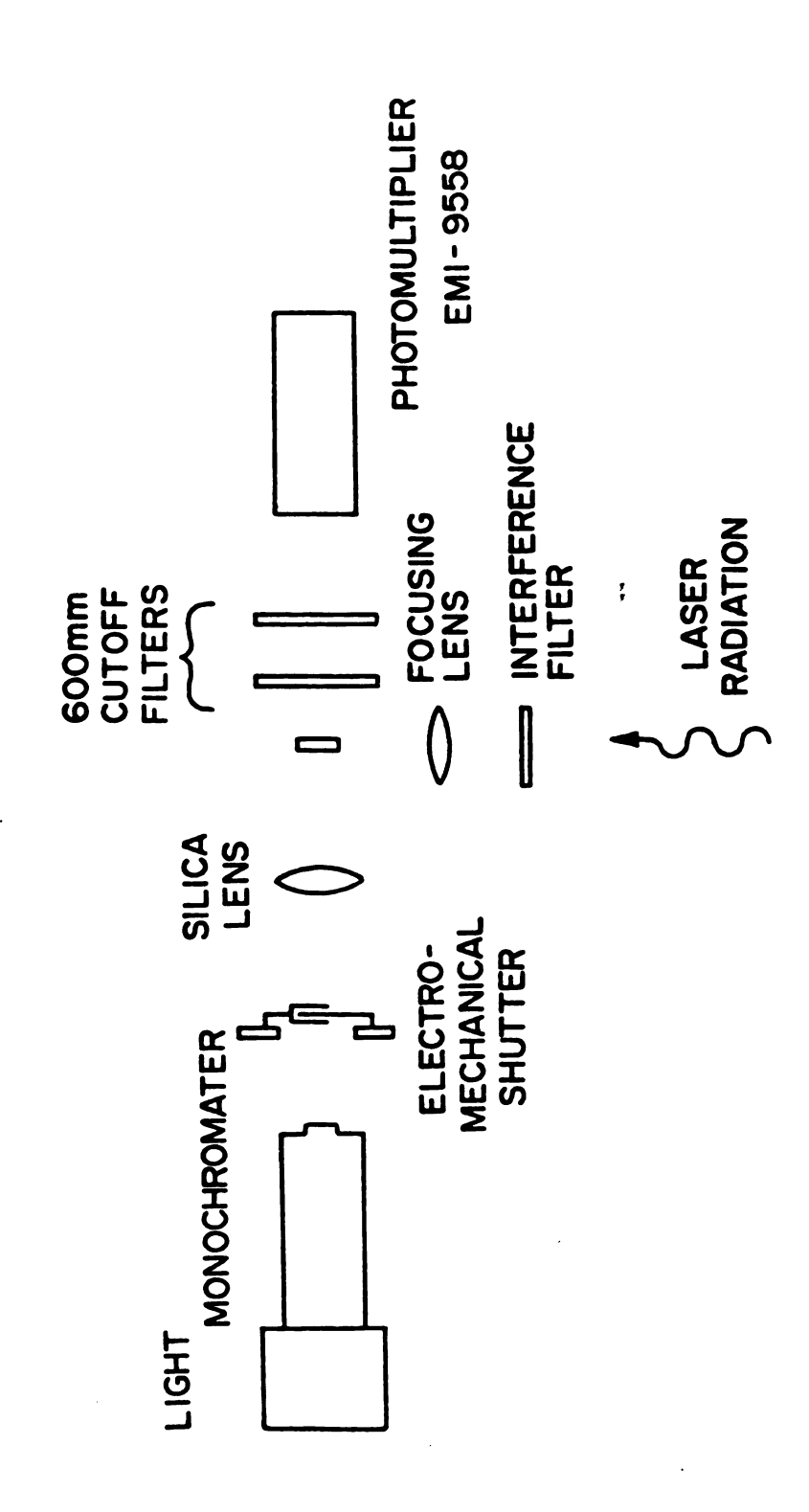
2.1 OPTICAL

The optical subsystem is as in Figure 2.1. All components (except for the PMT) are mounted on an optical rail bolted to a heavy length of colorlithe (lab bench material), secured to a lab bench top. This insures that high frequency vibrations will not cause mechanical instability in the optical alignment. A H-20 monochromator and a 100 watt tungsten light source (both from Instruments SA (ISA); Metuchen, NJ) are used to produce the collimated probe beam. ISA provides an alternating current (AC) variable power, 25 volt, 5 amp, supply for the tungsten light source, but it is completely unacceptable for high precision absorption measurements. Modification to produce direct current (DC) light was effected as in Figure 2.3 with the help of M. Rabb (MSU Chemistry Department's electronic design specialist) in

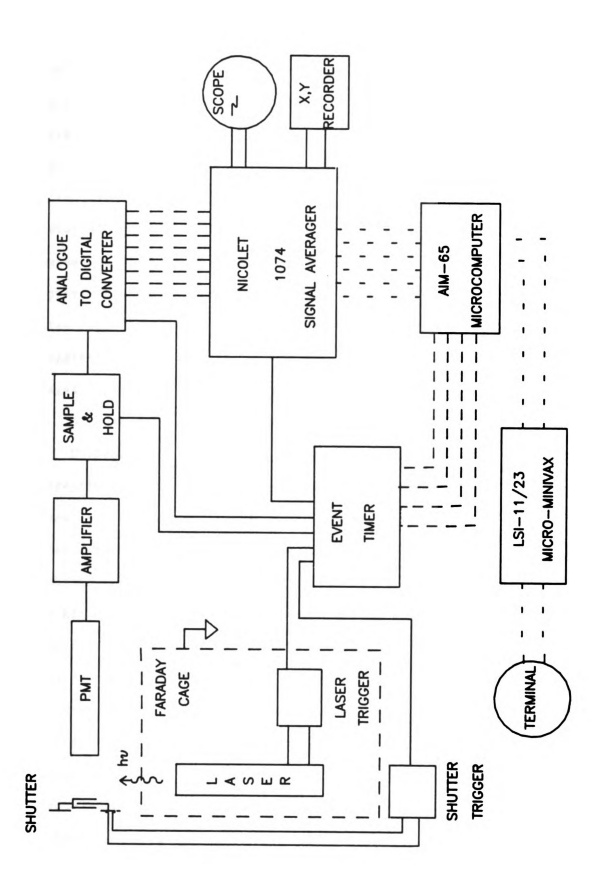
OPTICAL LAYOUT of the FAS. Only relative positions are shown, distances are not to scale.



OPTICAL LAYOUT of the FAS. Only relative positions are shown, distances are not to scale.



ELECTRONIC LAYOUT of the FAS. Analogue data pathways are given in solid lines, and the digital data lines are dashed. Only the electrical pathways are shown here. Note the electrical isolation of the Laser and it's trigger circuit; all other electronic components of the FAS run to a common ground (not shown).



locating a voltage regulator capable of handling the power output. The ripple (the amount of 120 Hz from full-wave rectification riding in a signal) in the current through the lamp is now less than 0.04% and essentially nondetectable by the PMT. The H-20 monochromator provides high throughput of light with adjustable bandpasses of 2,4, and 6nm which are suitable for flash absorbance studies. A mechanical photoshutter (Uniblitz, Model 100B, Advanced Electro-mechanical Engineering; Rochester, NY) protects the sample and the PMT from exposure to light during time delays. It is triggered by a positive TTL pulse and will remain closed or open indefinitely until a pulse "toggles" it to the opposite state. A focusing, fused-silica lens images light through the sample and onto the PMT.

A flashlamp-pumped dye laser (Phase-R Corporation, model DL-1100; New Durham, NH), rated for a maximum output of 250 mJ/pulse, is currently used as the excitation source. Rhodamine 640 when pumped lases at approximately 640nm. To insure dye stability and a pulse to pulse reproducibility of >90% the dye concentration is 5.0 * 10⁻⁵M in methanol, and the minimum time between any two flashes is ten seconds. Too high a dye concentration leads to a loss of output energy as rapid energy redistribution takes place among the dye molecules, and too low of a dye concentration leads to higher photolytic rates of decomposition of the dye and loss of power output. The long delay between flashes is necessary as the dye solution must flow down a 6" tube inside of the lamp. Flow rates are kept slow to minimize turbulence which would create inconsistent lasing conditions. Repeatedly lasing the dye without allowing for the tube to be purged and the dye to relax to the

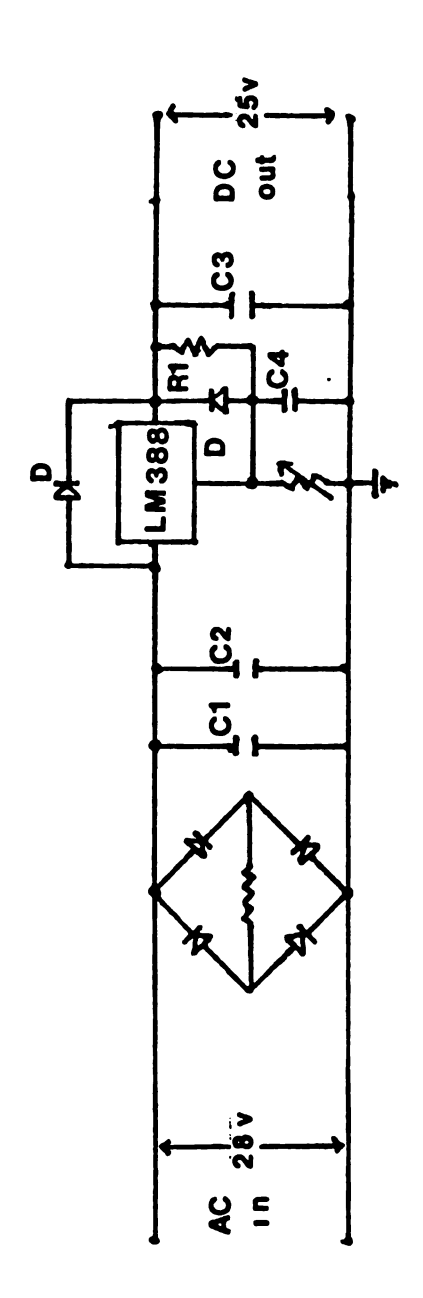
ground state also leads to high decomposition rates and inconsistent lasing action. An initial experiment on green plant photosynthetic systems (for experimental details, see Chapter Four) tested the saturation of photosynthesis, determined by the electrochromic effect at 518nm, as a function of the laser power output. Variation of the laser output by 50% still continued to fully saturate photosynthesis. The 600nm short-pass filter, the spectrum of which is shown in Figure 2.4, attenuates most of the exciting light at wavelengths higher than 600nm. Additionally, a 640nm interference filter is used in the path of the laser to eliminate white light components. Flashlamp-pumped dye lasers exhibit beam divergence due to a short cavity, thus necessitating two fused-silica focusing optics to focus the beam upon the sample cuvette.

The PMT is an EMI 9558QB (EMI Gencom Inc., venetian blind configuration, S-20 response; Plainview, NY) maintained at room temperature at a typical operating voltage between 530 - 800 V. The RCA 1P28 (RCA, side-on configuration, S-5 response; Lancaster, PA) was also tried. For the region of interest, 300 - 560nm, the 1P28 has a better ability to differentiate between the wavelength of choice and the exciting wavelength in terms of its response curve. At room temperature the 1P28 has less dark current than the 955QB; however, it was unable to detect the fast photosynthetic transients of interest.

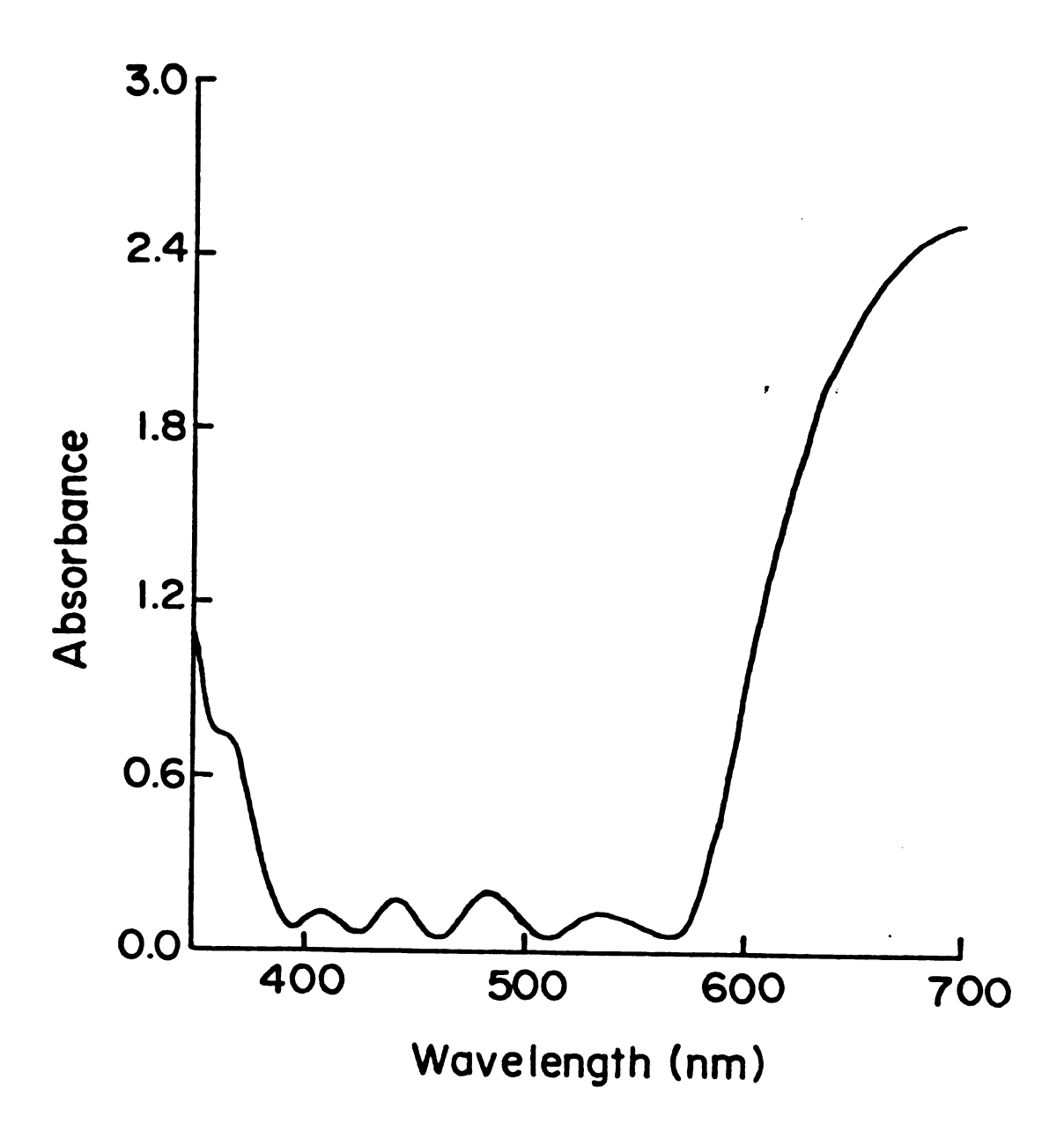
The initial configuration tried, separated the PMT from the sample cell by 200 cm. A quartz light pipe was positioned to receive all of the light from the sample and led to the face of the PMT where a silica lens was used to focus the light emitted from the light pipe onto the PMT. This set-up was used to insure that detection of exciting light

DC LIGHT MODIFICATION. This layout modifies the 28V AC current in to 25V DC

C1 = 2400 μ F; C2,C3,C4 = 10 μ F; R1 = 120 ohm; R2 = 5 Kohm, R3 = variable; D1,D2 = IN4002, protection diodes; LM338 5A,25V power regulator (National Semiconductor Corp.; Santa Clara,CA).



600nm CUTOFF FILTER SPECTRUM. Two such filters are used to guard the PMT from laser scattering.



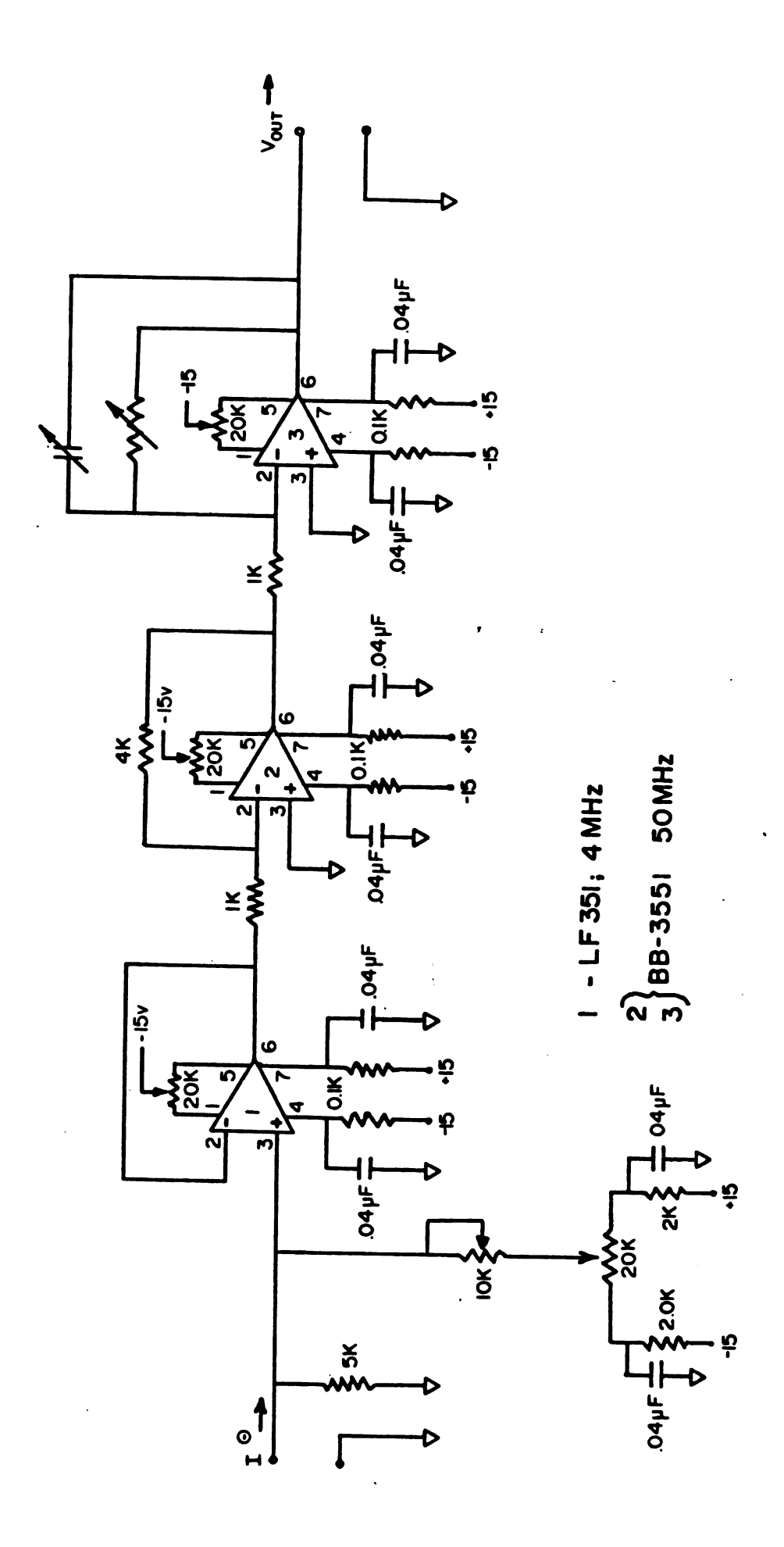
would be minimized; however, detection of the photosynthetic transients was also minimized. At present, 4.5 cm separates the face of the PMT from the sample cell. A new optical set-up is currently being built which will close the distance between PMT and sample cell to 2.5 cm. Requiring the space around the sample cell and PMT to be completely light tight (except for the exciting and probe sources), easy access to the sample cell, flexibility in choice of focusing optics, and easily added or removed blocking filters imposes severe design limitations, especially in terms of compactness.

2.2 ELECTRONIC

2.2.1 Detector Amplifiers -

The three stage amplifier circuit shown in Figure 2.5 is the final result of much modification and testing. Stages 2 and 3 use the BB3551 amplifier. Its GBP is 50MHz. Gain on the second stage is 5 thus giving a frequency response of 10MHz. The third stage is variable gain between 0.1 and 10; experiments usually use gains between 1 and 10. The first stage is a National Semiconductor LF351 (National Semiconductor Corp., GBP of 4MHz; Santa Clara, CA) set in a voltage follower configuration thus leaving the GBP equal to 4MHz. The typical frequency response of the system as a whole by Equation (1.26) is 2MHz. A faster amplifier in the first stage is preferred; however, tests I have performed (data not shown) indicate that the BB3551, if saturated for a short time (nanoseconds), displays a recovery time requiring several

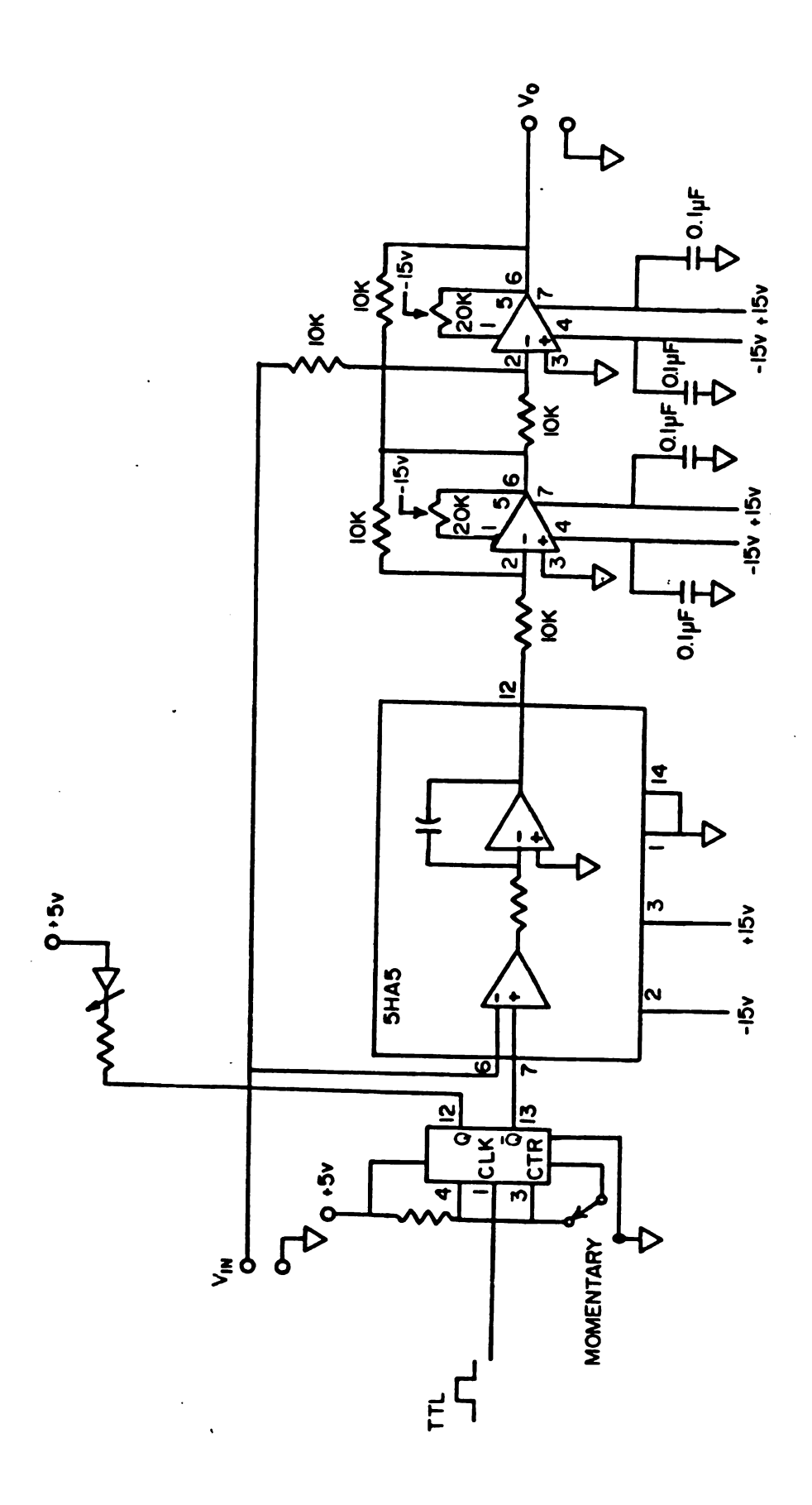
PMT CASCADE AMPLIFIER CIRCUIT. The first stage is connected to the base of the PMT by a 6cm long, heavily shielded, conductor. This is to reduce capacitance effects and pickup of Radio Frequency. The second and third stages are then housed in a separate box. Final output runs to a sample-and-hold amplifier. Adjustable gain on the thirds stage gives overall gains between 0.1 and 10,000. For a gain of 1, the adjustable time constant ranges between 3.8Mhz and 1Hz.



milliseconds. The LF351, while slower, recovers in nanoseconds from saturation.

Difficulty with single beam instruments are variations of the output DC voltage level owing to fluctuations over time (seconds) in power supplies of the PMT and the probe source, changes of the output the probe beam, component heating, sample distortion, etc. from Conventional double beam spectrometers resolve this problem by using a mechanical chopper and alternating between a signal and a reference, and correcting appropriately. In conventional single beam instruments the user has to set the OWT (transmittance) and 100%T by hand before making a measurement. A single-beam kinetic spectrometer, once operating, does not allow for readjustment of the ONT and 100NT before every flash, and analogue to digital (A/D) converters have a finite voltage range over which they convert. For optimal use of the digitizing range it is best to have the DC voltage level at 0.0 V. The detector amplifiers have a DC offset control which is set at the beginning of a set of flashes; however, the occurrence of slow fluctuations in the DC level are not compensated for and can drift out of the digitization range. A sample-and-hold (S/H) amplifier (Analog Devices, SHA-5; Norwood, MA) based automatic offset were developed (Figure 2.6) to eliminate these fluctuations. Ten milliseconds before the A/D converter is triggered to begin converting the S/H amplifier is triggered into a "hold" mode. The DC voltage level at that time is automatically subtracted out of all subsequent signals until another pulse is sent to the S/H to return to a "sample" mode. Over time scales short in relation with the slow variations in the DC level, the resulting output signal from the S/H is

SAMPLE-and-HOLD AMPLIFIER (S/H). The other two amplifiers after the SHA-5 are LF351s (not labelled). The input line is divided with one lead going to the SHA-5 and into the first LF351's inverting input, and the second lead ties up in a voltage summing configuration going into the scond LF351's inverting input. When the SHA-5 is in the "SAMPLE" mode it passes the input signal completely, it's inverted and summed with the positive signal for an output signal of 0.0V. When the SHA-5 is triggered into the "HOLD" mode it stores the voltage on a capacitor and holds that voltage on its ouput line, it is inverted, and subtracted from the preent signal resulting in an output signal centered around 0.0V D.C.



an accurate representation of the input signal minus only the DC level.

Absolute absorbances typically are not measured. I am usually interested only in the change of absorbance, ΔA , induced by excitation of the sample. Absorbance before excitation can be written as:

$$A_i = LOG(I_i^0/I_i), \qquad (2.1)$$

where A_i is the absorbance; I_i^0 , the radiant intensity upon the sample; and I_i , the transmitted or unabsorbed radiation. Similarly, after excitation

$$A_f = LOG(I_f^0/I_f). \tag{2.2}$$

 ΔA then is equal to the difference, $A_{\hat{I}}-A_{\hat{I}}$, or, expressed in terms of light intensities:

$$\Delta A = LOG(I_f^0/I_f) - LOG(I_i^0/I_i). \qquad (2.3)$$

Rearranging, and assuming $I_f^0 = I_i^0$, gives:

$$\Delta A = LOG(I_i/I_f). \tag{2.4}$$

The output of a PMT is proportional to the intensity of light; under the definition of the voltage offset, $V_{(off)} = I_i$, then ΔV is proportional to the change of light intensity, $I_f - I_i$:

$$\Delta A = LOG (V_{(off)}/(V_{(off)} - \Delta V))$$
 (2.5)

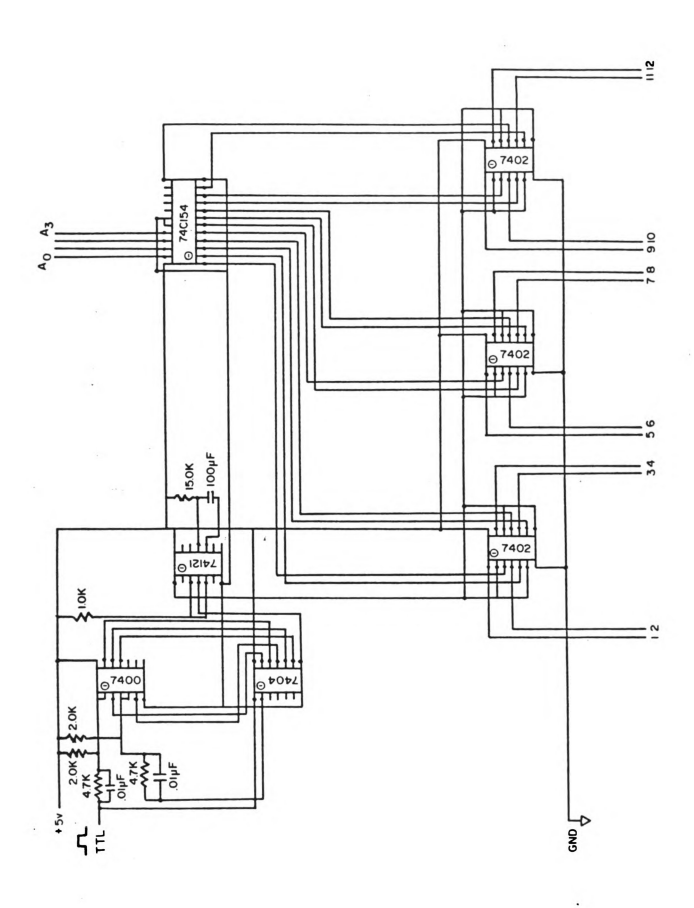
At the start of a series of flashes, the DC voltage is set to 0.0V and the offset voltage is set equal to $V_{(off)}$. ΔV is just the difference from 0.0V induced by the laser flashes.

2.2.2 Timing Circuitry -

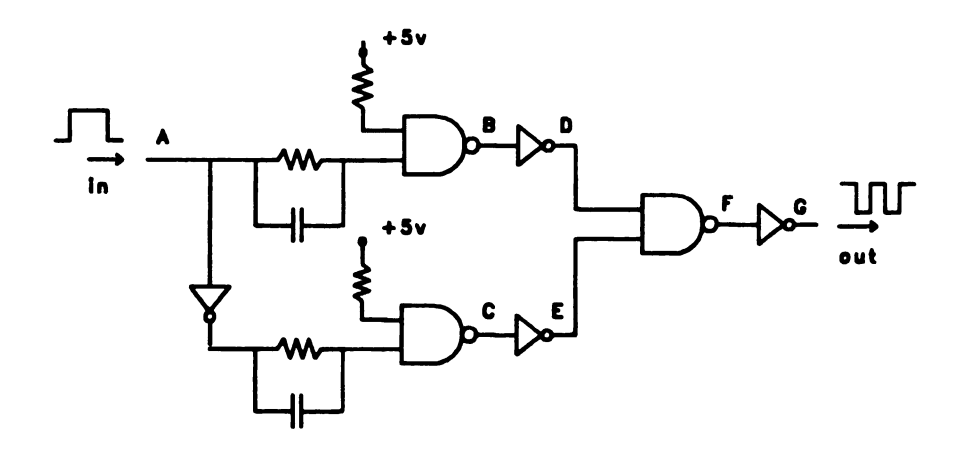
This circuit is the control interface between the computer (discussed below) and the discrete components of the FAS. Its layout is as in Figure 2.7. The computer provides four address lines for the decoder and a line which a "timer" toggles "HI" (+5.0 V) and "LO" (0.0 V) under software control. The rising and falling edges of each pulse are shaped into pulses used to trigger a monostable to send out a 1.5 µs negative pulse (see Figure 2.8) which is connected to all the NAND gates. Meanwhile the decoder selects one of its output lines to send "LO"; the NAND gate with both inputs selected "LO" would produce a "HI" output pulse for 1.5 us on the appropriate pin. A timing schematic is as shown in Fig 2.8, minimum time, as dictated by hardware, between pulses is 2.5 µs; maximum time is undefined. This interface has twelve lines going out, with room for four more if the current circuitry is used, and provides immediate and interactive control over any device requiring a standard TTL pulse.

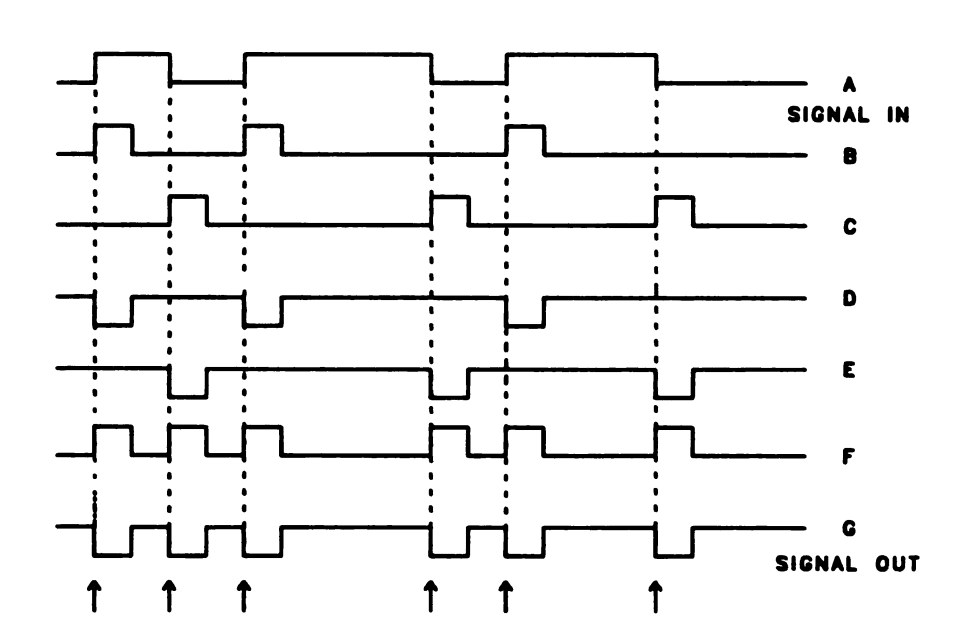
A cautionary note is in order here. If any of the external devices develops and reflects down its control line high voltage/frequency spikes, or if the control line acts as an antenna and picks up these spikes, this will affect the integrity of the interface, other devices, and the computer itself. The Phase-R laser is renowned for this as well as its RF (radio-frequency) interferences, and has been throughly grounded, shielded, and isolated as described as in (25).

TIMING CIRCUITY. The AIM-65 is required to bring four address lines, AO - A3, and a timing line (labelled TTL), in to run the circuitry. The 74C154 is a 4 to 16 decoder and provides 16 discrete output lines (only 12 are currently utilized). The 7400 (NAND gate) and 7404 (HEX INVERTER) are used to shape each transitions on the TTL line into pulses (detailed description in text and logic involved in FIGURE 2.8). A monostable vibrator (74121) trims the pulse duration to 2.0 µs, and the output is fed into input of each of 7402 (NAND gate). The NAND gate selected will be the one which has its input line from the decoder LO; when the other input, from the monostable, goes LO it will produce an output HI pulse of the same duration as the monostable's.



TIMING SCHEMATIC. The logic involved in transforming each transition (LO -> HI or HI -> LO) on the input TTL line, A, into a final output line, F, with one pulse per transition. The output of each gate is labelled and is matched with a time trace below.





2.3 COMPUTER

2.3.1 General -

Three computers are directly involved in the operation of the FAS, and a fourth if extensive numerical computation or high precision is required. Immediate data storage is provided via a modified (discussed below) NICOLET 1074. Instrument control is provided through a ROCKWELL AIM-65 micro-computer. Long-term mass storage and data processing is provided by one of two DEC (Digital Equipment Corporation) PDP-11 (either /02 or /23 processor) minicomputers.

Each will be discussed in turn below.

2.3.2 Nicolet 1074 -

The NICOLET 1074 (Fabri Tek, equipped with an SD-72/2A 9-bit A/D converter and a SW 71A sweep controller; Madison, WI) is of early to mid 1960's wintage, and contains four memory channels of 1,024 bytes (commonly referred to as "1K") where a byte represents a data point of an arbitrary integer

representation of less than 2^9 and greater than $-(2^9)$. The internal 9-bit A/D has a dwell time of 20 μ s per point for 1024, 2048, or 4096 bytes (or points) sequential in time. Modifications by C. Yerkes, B. Buttner (members of the Babcock Laboratory), and M. Rabb enabled direct addressing of the NICOLET's data registers from an external source. This allows use of external A/D, with dwell times between 60 ns to 10 us for a total of 1023 points, to write into a selected memory channel of

the NICOLET. Other modifications include multiplexing ability which permits 4 sequential triggers to be loaded into the four memory channels. This is an ideal feature for experiments looking for periodicity of less than or equal to four.

Principal use of the NICOLET is as a signal averager; repeated triggering causes the new data set to be summed with that already existing. It also contains the hardware to maintain a "current status" of the data contained in its memory on an oscilloscope, provide hard copies, scaling, and some elementary arithmetic processes. Duplication of these features in the AIM is feasible, but the overall performance of the AIM and the system as a whole would be degraded severely.

2.3.3 AIM-65 Microcomputer -

Tending the timing device circuitry and the NICOLET is the AIM-65 microcomputer, which serves as essentially the "brain" of the system. The AIM-65 is a single-board microcomputer which is extremely flexible owing to its design as a system development unit. The heart of the hardware is an 8 bit 6502 microprocessor unit (MPU) with a clock frequency of 1MHz. The AIM, in its present configuration, has an 8K ROM (read only memory) ASSEMBLER, 8K ROM BASIC interpreter, 4K RAM (random access memory) for programming, and a 4K ROM MONITOR and EDITOR. Memory expansion up to 64 K is accommodated through its parallel expansion connector (not yet implemented) and device interfaces through its parallel applications connector. An onboard keyboard, 20 character display and 20 column thermal printer, and 2 FSK (frequency-shift keyed) cassette lines allow this MPU to be used in a truly "stand-alone"

environment. Use of a cassette recorder as a mass-storage device was quickly discarded in favour of using the PDP-11. As the AIM provides for an off-board use of a terminal, a circuit (73) to convert the 20 mA current loop to a standard RS232 was built, and all communication to the AIM is now accomplished through a Zenith Z-19 terminal and/or the PDP-11.

Two parallel ports, A and B, of 8 lines each with a variety of control lines for "hand-shaking" reside in the applications port. Port B also is connected internally to a user-definable R6522 (Versatile Interface Adapter, Rockewll Int'l. Corp.; Anaheim, CA. For general usage and detailed explanation of operation see (74).), a integrated circuit chip containing two 16 bit timers which run at a clock frequency of 1MHz. Timer 1 of the 6522, PB7 (Port B line 7), can be software configured to invert the voltage on PB-7 each time it completes a countdown. An automatic reloading feature permits the user to set the timer running and then to load a new time into the latches of the timer without affecting the current timing setup. Completion of the count inverts the voltage level, automatically loads the new time, and sets an interrupt. Four other lines of Port B (PB-0 - PB-3) are used to select the correct addresses for the decoder in the timing circuit.

Port A is used for data transfer from the NICOLET to the AIM and subsequently to the PDP-11. The data is encoded in inverted binary coded decimal (BCD) logic in coming up from the NICOLET to the AIM, translated into ASCII code and is sent in a serial fashion to the PDP-11. A full memory transfer from the NICOLET requires 90 seconds (the initial version of the data uploader was written in BASIC and

required 20 minutes) at 9600 band (9600 bits per second)

The PDP-11 is thus used as a mass-storage device during experimental runs, and later for data analysis. Initial analysis consists of automatic file documentation which provides a safeguard for experimental parameters, and conversion of initial raw voltage data into absorbance data. Each data file is fully compatible with the Chemistry department's CEMCOMGRAF facility as well as the more limited facility of the Babcock Laboratory; additionally each file is structured to be amenable to a more sophisticated data-base management protocol currently being developed. Additional processing is available through a prototype data file handler developed during the course of this work and discussed in more detail in the next Chapter.

For high-precision computations or cases where numerical overflows are likely (PDP-11 computers are limited to -10^{37} and 10^{37}) a modem link to the University computer can be used to transfer data to take advantage of the higher precision and greater numerical range.

CHAPTER 3

SOFTWARE DESIGN

3.0 PROGRAMMING CONSIDERATIONS

Microcomputers have languages available to them from the high level ones such as BASIC or FORTRAN, intermediate ones such as FORTH, and low-level machine language (Hereafter loosely referred to as: ASSEMBLY.). Many commercial instruments which allow user interaction and control through specific application programs provide some form of BASIC.

For applications where program execution speed is critical or where memory limitations are severe have forced most control programs to be written in ASSEMBLY. BASIC as an interpreted language is far too slow, FORTRAN requires large amounts of memory and/or mass storage, and compiled BASIC suffers from the same limitations as FORTRAN.

For environments in which the microcomputer is not forced to function as a stand-alone system and can interact with a larger "host" system, the software development phase can be done on the host and the programs then transferred into the smaller microcomputer. This type of implementation is used extensively in the MSU's Chemistry Department. The interactive language largely used

is FORTH which executes much faster than BASIC and occupies much less memory. FORTH is also advantageous in that execution speed critical code can be written in

ASSEMBLY in the body of the main program, not requiring the programmer to go through the tedious task of "linking" together the various program segments. BASIC has been used in this particular implementation rather than FORTH for two reasons. Initially BASIC was the only high level language offered for the AIM-65; therefore, initial programming was done in this language. Second, more scientists are fluent in BASIC instead of FORTH; thus comprehension and modification of the program by others will be an easier task than if written in a relatively obscure language.

Another way to address the host-microcomputer interaction is through a "master-slave" interaction, which is standard for most typical computer peripherals such as lineprinters or terminals. In this instance the peripheral, in this case a microcomputer, is given enough ability through hardware and permanently implanted programs in ROM to perform very specific tasks. Interaction with it is through the host computer only. An immediate effect of this is a reduction in the memory size the microcomputer programs require as terminal drivers and other input/output (I/O) routines are no longer required.

Appendix A contains a listing of the three routines with their inline documentation used in the AIM-65.

3.1 AIM-65

3.1.1 System Execution -

At the expense of memory, the main routine has been written to give informative prompts and error messages as necessary. Upon loading and

running the system, the user is queried as to the function to be performed, new or old timing setup, data uploading, or exiting. New timing setups reinitialize all memory cells used for data storage. The user is then prompted for the number of pulses to be sent, number of cycles. For each pulse the user is requested to enter a device name, time (in microseconds), and the address requested. For both old and new timing setups the integrity of memory is checked, and error messages are generated and execution halted if needed.

Operation of the Kinetic Operating System can be through the PDP-11 or as a stand-alone system. Only in the case of data uploading is actual linkage to the host computer required. The system is general and quite versatile in its timing functions.

3.1.1.1 Program Description -

Three programs provide the necessary hardware timing control, data uploading, and interactive with the user. Program listings with in-code documentation are in Appendix A. Brief descriptions of their functions follow.

KOS.BAS is the BASIC routine which provides the user with a limited number of options, initialization of memory regions according to the option selected, and interactive querying for necessary information to fulfil the option. Most microcomputer BASIC interpreters allow for linkage to user written assembly routines. The requirements for this linkage involve placing into specific memory cells the "vector" or address pointing to the start of the program; then a function call similar to: I = USR(NUM), is executed. "NUM" is a floating point

number passed directly to the Assembly routine. Microcomputer development systems are limited in readily available utility programs (i.e., there are none) for aiding software development; thus, linking loaders (programs which are capable of taking several separately developed inter-dependent programs, resolving addressing differences, and loading them into memory as one program) are nonexistent, and program linkages are the user's responsibility. Modifications to assembly programs usually change starting addresses, sizes, etc.; therefore, an implementation which has been adopted here, to minimize the number of program(s) modifications each time a single program is modified, is to place at the top of memory the starting address of variables and of the code itself. KOS is thus required only to PEEK (a function permitting direct examination of memory through BASIC) to find the starting address, place them in the JUMP handler, and then to execute a function similar to the above.

This protocol requires fewer changes than otherwise, and suffices in the absence of a relocatable assembler and linking loader.

KOSTIM. AIM is an assembly routine which executes during the timing sequence under interrupt control, and directly controls the timing circuitry. The timer, the R6522, is only a 16-bit timer providing a maximum of 65536 µs between completions (.066 seconds). To circumvent this restriction a third byte is kept in memory which KOSTIM decrements each time the timer completes its count. When the third byte reaches zero, KOSTIM advances to the next devices's timing delays, loads them into the timer's latches, and continues as before. Three bytes for specifying a time gives a maximum of 16.7 seconds between pulses, and

the increased overhead in program execution raises the minimum time between pulses to 150 us. When the third byte is used the timer still times-out and toggles PB-7, but all possible device addresses will be de-selected except on the last time through the iteration. An earlier version printed out the number of iterations completed, but the AIM uses the second timer of the 6522 for band rate generation and a hardware interference exists between the two timers causing inaccurate timing sequences. At present data storage exists for 24 TIL pulses to be sent out per cycle for 255 cycles. No restriction exists on which of the TIL outputs is selected nor how many times in a cycle.

Transfer rates from the NICOLET through the AIM to the PDP-11 is close to the maximum that an PDP-11 floppy drive based system can handle. A recent upgrade to an RSX-11M multi-tasking/user operating system cannot support this high transfer rate.

KOSNIC.AIM is an Assembly program which uploads the data from the NICOLET and handles the output directly to the PDP-11 itself. Memory constraints require that data transfer from the NICOLET occur on a number by number transfer of nine bytes per number

3.2 LSI-II/02-23

HALCDC.MAC (65) was initially written for use with a CYBER-750 and allows the PDP-11, operating under an RT-11 operating system, to function as a terminal emulator while retaining the ability to pass or receive data locally. Relatively extensive modification permits CDC to serve as the interface link between the PDP-11 and the AIM. Data transfer rate between the two is at 9600 baud (960 characters per

second). The major detriment to this arrangement is the monopolization of the PDP-11 during the course of the experiment due to the restrictions of the RT-11 operating system. Recent computer hardware upgrades allows use of RSX operating systems; however, CDC will require further modifications, as of this writing, to function in a multi-user environment. Data conversion and manipulation is performed by KINSET.FIN and MINI.FIN. MINI converts data files uploaded, each of which consists of only time sequential lists of voltages, into files maintaining the initial raw voltages, the corresponding time (in micro-seconds), and the change in relative absorbance as calculated by equation 2.5.

MINI prompts for the necessary information and for all additional experimental parameters, performs the necessary conversions, and stores the data in an unformatted binary sequential file. All of the records containing parameters of the experiment are "tagged" with "DO", and all data records with "RD." This file serves as a"unit" for a future data base implementation and helps to insure that experimental parameters will be retained. The file created is compatible with MULPLT, the Chemistry Dept.'s Graphics Facility maintained by Dr. Tom V. Atkinson, as well as the more limited graphics facility which has been implemented during the course of this work on the Babcock laboratory's PDP-11.

KINSET.FIN is a generalized file handling program developed here. It's initial implementation in a PDP-11/02 RT-11 system was limited to performing arithmetic operations between two files and some manipulation of the data within a file. A recent upgrade to the PDP-11/23 RSX-11M system takes advantage of virtual array space and faster disk access

times. It's operations are on or between fields of data, where each field is a complete set of x,y data (an inclusion for individual weighting of each datum will be in the next upgrade). Operations on a field include base-line corrections by variable order polynomial fitting, multiply, divide, add, and subtract functions, numerical differentiation and integration, and various smoothing algorithms. Operations between data fields are limited to the four basic arithmetic functions. Windowing, terminal plotting, listing facilities, and several file output formats are available. This program, in effect, eliminates the need for most specialized data manipulation and conversion routines typically found in scientific environments. Dynamic display and handling of large quantities of data can give one a "feel" for the data, and better insight into solving particular experimental or model problems. The next version will include Fourier and Inverse Fourier transforms, digital filter techniques for enhancing signal to noise ratios, spline fitting algorithms for interpolation and extrapolation, and an increase in data base size. A fourth program, CFIT.FIN is a completely general non-linear parametric-fitting program implemented for kinetic analysis on a PDP-11 computer system. CFT4A.FTN (35), a subroutine, has been modified to serve as the "algorithm" unit for CFIT. While CFIT is useful for small sets of data (less than 100 points), hours can be required when fitting a set containing 100 points; therefore, its overall usefulness is

limited owing to a relatively inefficient "minimum-seeking" algorithm in CFT4A, and slow processor cycle times of the PDP-11 compared to the CYBER-750.

CHAPTER 4

EXPERIMENTS AND FUTURE PLANS

4.0 MATERIALS and METHODS

4.0.1 Chloroplast Preparation -

Class II chloroplasts were used in all experiments described in the following sections, and were prepared as according to Robinson et al. (23) and briefly summarized here. Commercially available spinach was washed and depetiolated (leaves separated from the stem). The leaves, 500-1000 grams., were ground in "Grinding Buffer", a solution of 0.4 M NaCl, 2 mM NgCl₂, 1.0 mg/ml Bovine Serum Albumin (BSA), 1 mM Ethylenediamine tetraacetic acid (EDTA), and 20 mM HEPES at a pH of 7.6, for 10 sec in a Waring Blender. The homogenate was then passed through 8 layers of cheesecloth; the supernatant centrifuged until 3500 x g was reached and then stopped. The supernatant was then resuspended in the "First Resuspension Buffer", a solution of 150 mM NaCl, 4 mM NgCl₂, and 20 mM HEPES at

a solution pH of 7.6, and centrifuged at 7500 x g for 10 min. After centrifugation the pellet was resuspended and stored in SHN, a solution of 0.4 M Sucrose, 10 mM NaCl, 50 mM HEPES at a solution pH of 7.6.

Chloroplasts were stored typically at -40°C with no apparent loss of photosynthetic activity; however, the question of membrane integrity

is taken up later.

Final chloroplast concentration as function of chlorophyll concentration was determined as by Sun and Sauer (24). Chloroplasts were diluted 1:200 into a solution of 80% acetone/20% H₂O, filtered, and absorption at 652 nm measured in a 1 cm cell. Concentration in mg Chl/ml was determined by multiplying absorbance by 5.8.

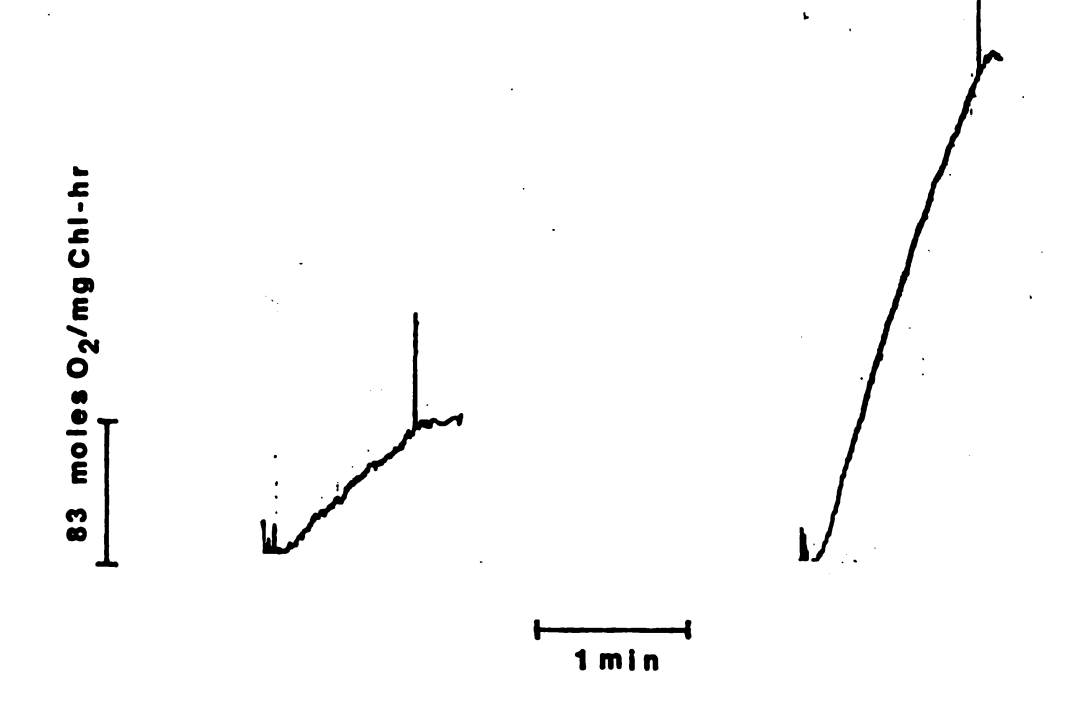
Photosynthetic activity and integrity were assayed at time of preparation and before each experiment by measuring steady state rate of oxygen evolution. Method and apparatus were developed in the Babcock laboratory by Yerkes (25) and Buttner (26). Chloroplasts were diluted to 70 ug/ml in a solution of 50 mM NaCl, 2 mM MgCl₂, 20 mM HEPES, and 3.6 mM K₃Fe(CN)₆ (an electron acceptor) at a solution pH of 7.5. Equilibration for 30 sec preceeded the actual measurement. Two sets of measurements were always made; the first as above measuring the "coupled" rate of oxygen

evolution of with the addition of methylamine, $CH^{3s}(2)$, to a concentration of 10 mM, as an uncoupler, measuring uncoupled oxygen evolution. Uncoupling usually stimulates the rates by three to four fold. Figure 4.1 shows typical traces of coupled (4.1A) and uncoupled (4.1B) rates over the same period of time. This procedure provides a crude estimate of the intactness of the entire photosynthetic

[&]quot;1)"In this context coupled oxygen evolution means that the entire photosynthetic chain from the OEC to the ATPase is operational. Water is being oxidized and ATP is being produced. Uncoupling permits the OEC to continue to oxidize water, but ATP is no longer produced.

OXYGEN EVOLUTION. This depicts typical oxygen evolving rates seen with class II chloroplasts prepared as described. These rates were obtained with freshly prepared chloroplasts. Rates obtained with freeze-thawed chloroplasts (not shown) are similar. (A) Coupled oxygen evolving rate.

(B) Uncoupled oxygen evolving rate.



apparatus from the OEC to the ATPase. Only chloroplasts with uncoupled rates of greater than 200 μ moles O_2/mg Chl·hr were used.

TRIS-washed chloroplasts, while not used in any of the experiments described herein, are planned for some experiments and are used in many of the experiments described in the literature, and are thus described here. TRIS-washing is perhaps the mildest known treatment for inhibiting oxygen evolution. The preparation of TRIS-washed chloroplasts is as above except for two additional suspension and centrifugation steps. After the second centrifugation (described previously) the chloroplasts were suspended in a solution of 0.8 M TRIS, and 1.0 mm EDTA at a solution pH of 8.0, and incubated under room light at 4°C for 20 minutes. Afterwards they were centrifuged at 4000 x g for 10 min., the pellet resuspended in the first resuspension buffer, centrifuged at 4000 x g for another 10 min., and finally suspended and stored in SHN as described above.

4.0.2 Standard Experimental Conditions -

Standard class II chloroplasts, evolving greater than 200 μ mole $0_2/mg$ Chl·hr, were used at a typical chlorophyll concentration of 49 μ M in a total solution volume of 1.5 ml. A quartz cell with 0.5 cm path length held the sample positioned before the PMT in the path of the probe beam. Monochromator bandpass was usually 4 nm. PMT voltage was between 530 - 600V.

Recalling Figure 1.1, NADP⁺ is the final electron acceptor in vectorial electron transport through the two photosystems. Chloroplast preparation, however, disrupts the ferredoxin-NADPH reductase complex

which interfaces the one-electron chemistry of ferredoxin with the two-electron reduction of NADP⁺. This entails the need to add exogenous electron acceptors to the reaction media. For experiments requiring operation of both photosystems Methyl Viologen (MV) is often used as it removes the electrons from PSI. For experiments involving only PSII DCMU and ferricyanide can both be used together. DCMU blocks electron transfer between Q_a and Q_b , and prevents PSI from operating. Ferricyanide accepts electrons then directly from Q_a , albeit slowly.

Reaction media was typically SHN except for experiments involving proton release/uptake measurements. Reaction media experiments involving proton measurements consisted of 10 mM KC1, 2 mM MgCl₂, and (if present) 1.0 mg/ml BSA at a solution pH of 7.6. Electron acceptors were as described (above).

A typical timing sequence is depicted in Figure 4.2. Generally, the sample was exposed to the probe beam 50 ms before triggering the S/H, A/D, and Laser to allow settling time for the PMT. Immediately after conversion ends the S/H reverts to "sample [" mode and the shutter is closed to reduce perturbational effects from the probe beam. Total exposure time throughout the entire experiment was no more than 1.0 sec.

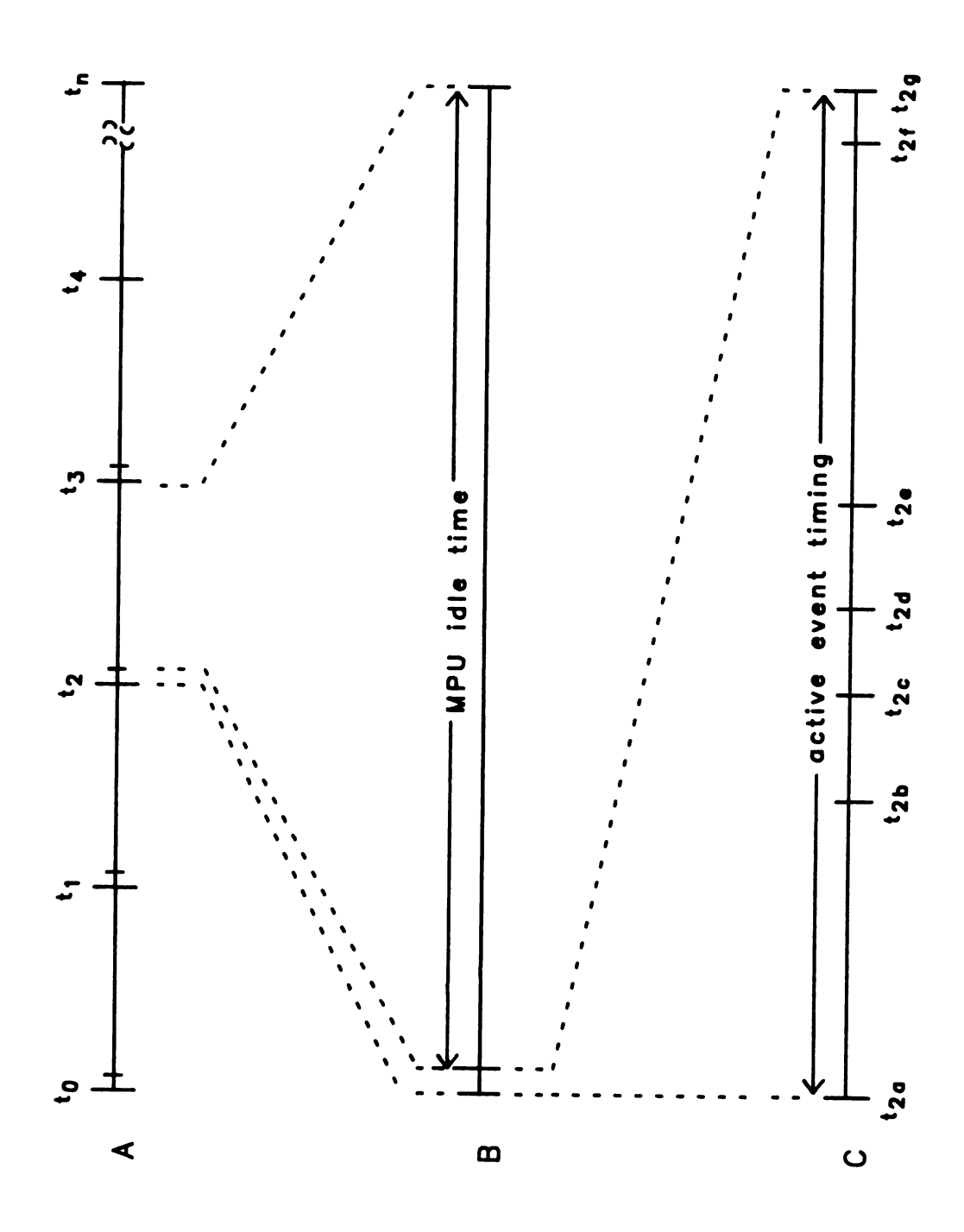
4.1 CONTROL EXPERIMENTS

4.1.1 Steady state effect of Probe Beam -

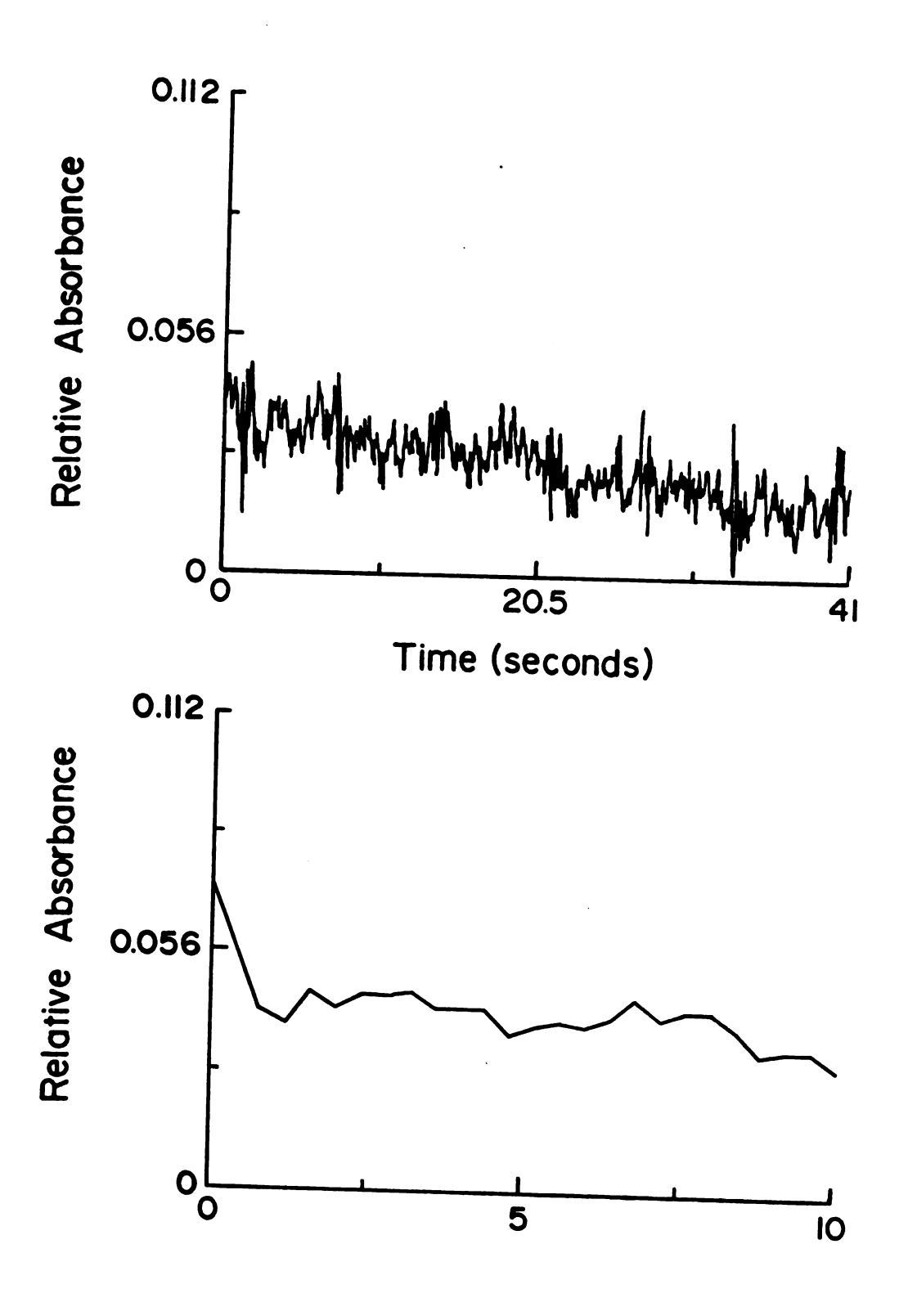
Figure 4.3A shows the effect of the probe beam continuously illuminating a standard sample in which both photosystems were

A typical sequence of timing events (not to scale). On the top line, A, each t_i indicates the beginning of a timing cycle. The cycle repeats itself at every t_i . the smaller line after the t_i marker indicates that the active event timing is completed, and the AIM-65 enters an idle loop until the beginning of the next cycle. Line B is an expansion of one cycle, and line C is an expansion of the active event timing portion. Example times are given below (note: all times are given with respect to the previous event):

time	duration	event			
tia tib tic tid tie t1f	50ms 10ms 0-1ms	<pre>photoshutter open S/H - 'hold' A/D - begin converting</pre>			
t _{id}	1-20ms	NICOLET - begin storage			
tie	10ms 1ms	S/H - 'sample' photoshutter close			
t _{1g}	1-15:	enter idle loop			



PROBE LIGHT EFFECT. The effect of continous illumination of the sample by the probe for: (A) 40.92 seconds, and (B) 1.0 second.

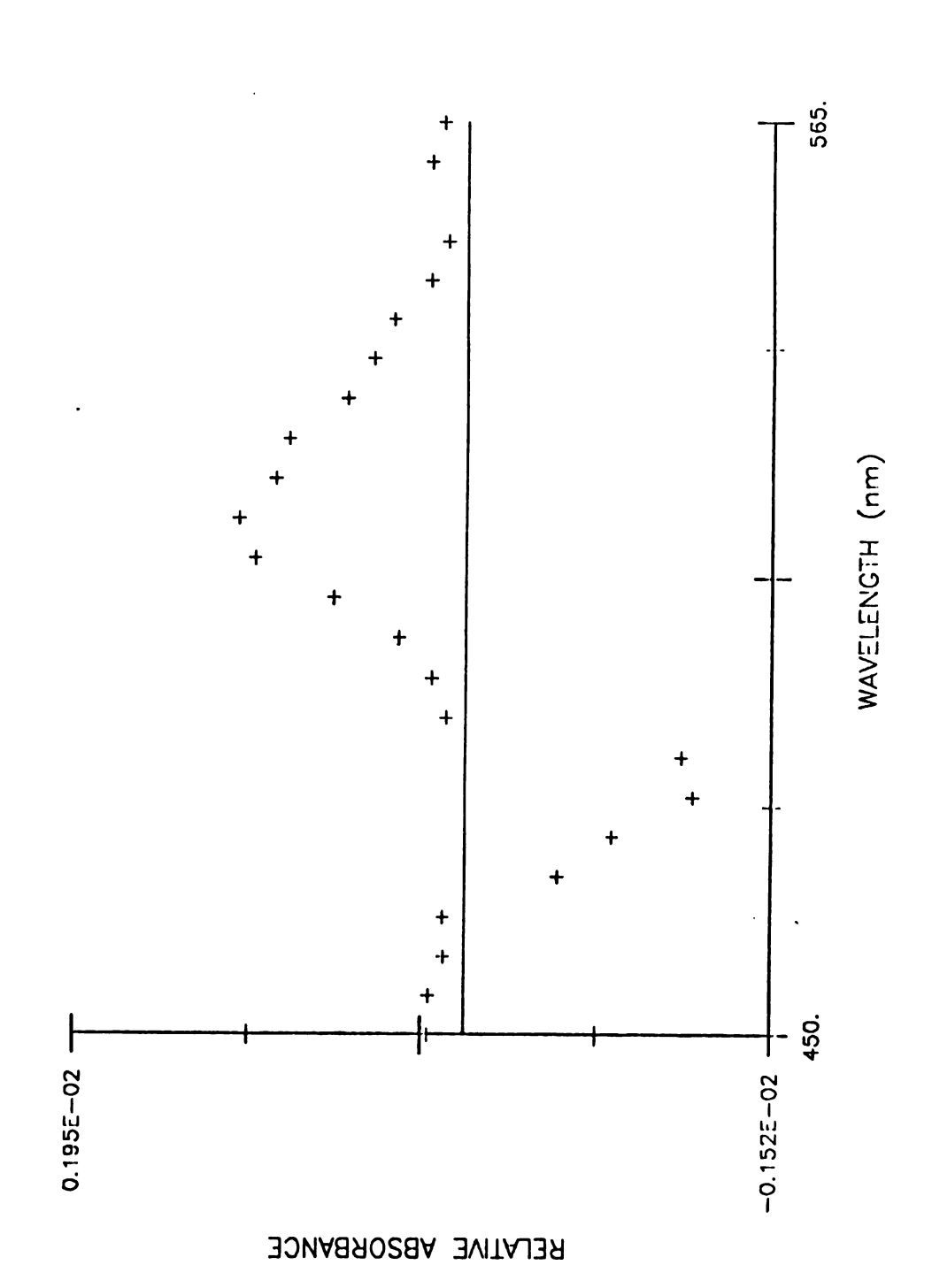


operational for 40.9 sec, and Figure 4.3B is the same for 1.0 sec. An overall decrease in absorbance is seen over 40.92 sec; however, photochemistry induced by the probe beam is expected to increase the absorption. Clearly, what is happening is that the sample is settling and decreasing the absorption. Figure 4.3B reveals no significant change in absorption. The noise level is high as the time constant for this particular trace was less than 10 µs.

4.1.2 Flash-induced Difference Absorption Spectrum discussed in Chapter One and depicted in Figure 1.5, the effect of an absorption band shiftis the derivative of the absorption band. Chloroplasts this shift is observed from 400-570nm. Figure 4.4 is a plot of a flash-induced electrochromic difference spectrum and follows the expected derivative shape. Two measurements, each consisting of 25 flashes spaced 10 seconds apart, were made to obtain each point. Both measurements were taken under standard conditions, excepth that the second included 5 µM Gramicidin. The second set of data would then contain the same set of absorption changes as the first except for those due to the electrochromic effect. Subtraction of the two sets of data would according to Equation (4.1): eqtabl eqon $\Delta(\Delta A) = -(\Delta A_{a+d} -$ (4.1) eqoff where $\Delta(\Delta A)$ is the difference in relative absorbancies; ΔA_{std} the induced difference with no chemical modifications of the electron

transport chain; and ΔA_{grm} , the induced difference with Gramicidin to eliminate the electrochromic responses would yield a flash-induced electrochromic

FLASH INDUCED DIFFERENCE ABSORPTION SPECTRUM. Center line represents zero absorption changes. Each "+" marks one point.

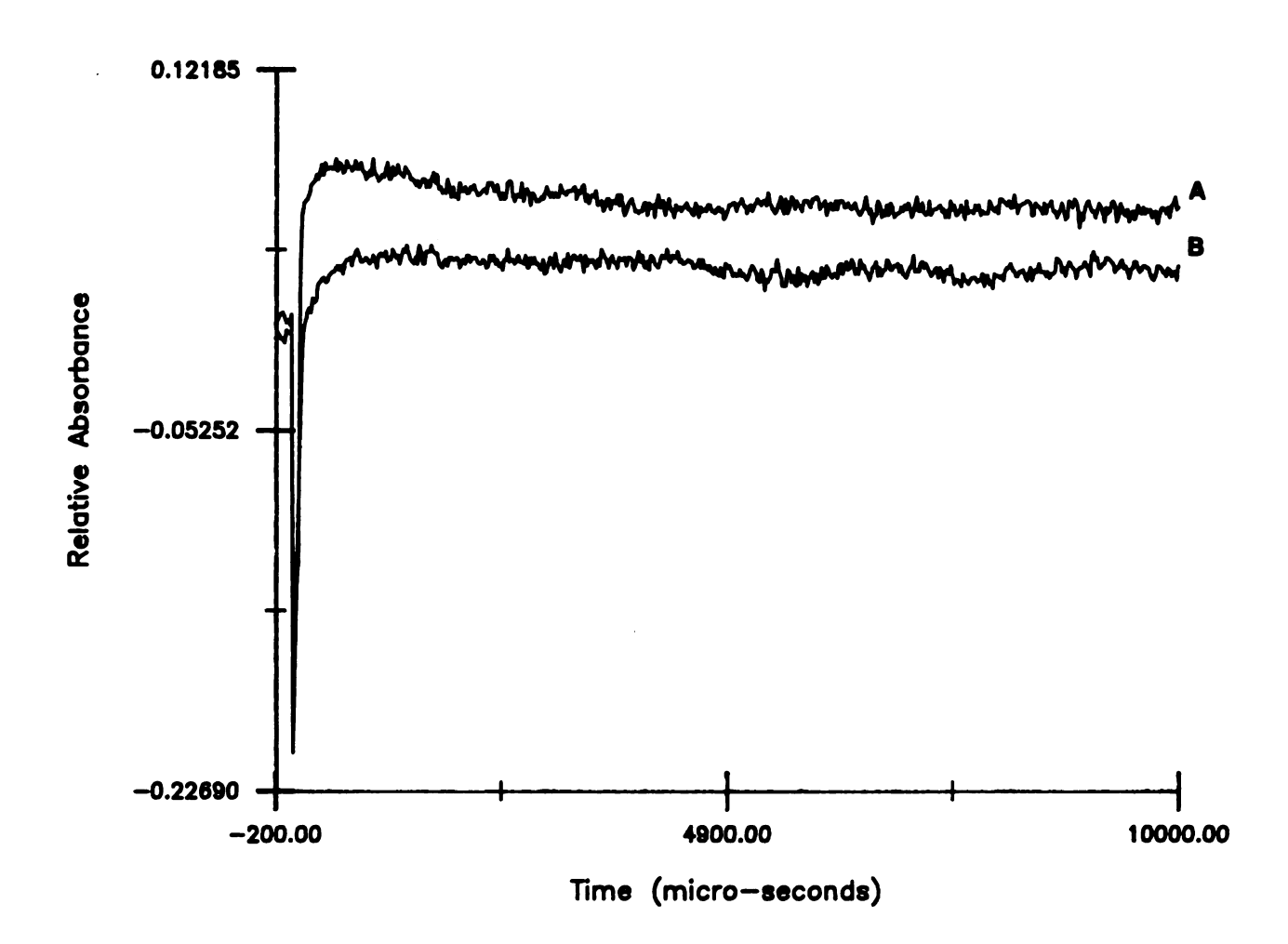


spectrum. As discussed, in Chapter One, the electrochromic response is a result of the electric field set up by the charge separation across the membrane. Gramicidin in nanomolar and above quantities causes the membranes to become ion permeable, and allows rapid decay of ion or electrical gradients through high ion fluxes. This results in almost immediate collapse of the charge separation and, rapid decay of absorbance changes due to this effect.

4.1.3 Effect of DCMU on the 518 mm change -

As discussed previously in this chapter, if ferricyanide is used as an electron acceptor and DCMU as a blocker between Q_a and Q_b then only PSII is operational, the result of this is that only PSII contributes to the trans-membrane charge, i.e., only one half of the normal charge should be generated across the membrane. The electrochromic absorption change at 518nm should then be one half of that normally seen. Figure 4.5 reveals this to be so. Two traces with their baselines superimposed at the time of the flash, are in Figure 4.5. both were taken under standard conditions, 25 flashes each with 10 seconds between flashes. Trace B has had 166 µM DCMU added. Higher concentrations of DCMU did not decrease the response in DCMU-poisoned chloroplasts. Lower concentrations of DCMU lessened the effect. The amplitude of trace A is double that of trace B. This is in agreements with Hong et al.(55), Schliephake et al.(56), and Joliet et al.(77).

EFFECT OF DCMU ON 518 CHANGE. Baselines of the two traces shown were overlapped to emphasize the difference in absorption changes. Trace A is a normal 518 change, and trace B is the response with 166 μ m DCMU. The negative spike(s) are at time zero, and is the PMT's response to the laser excitation. Time constant was less than $5 * 10^{-6}$ sec, [DCMU]=166 μ M, [MV]=49 μ M, and equilibration for 60 seconds was allowed.



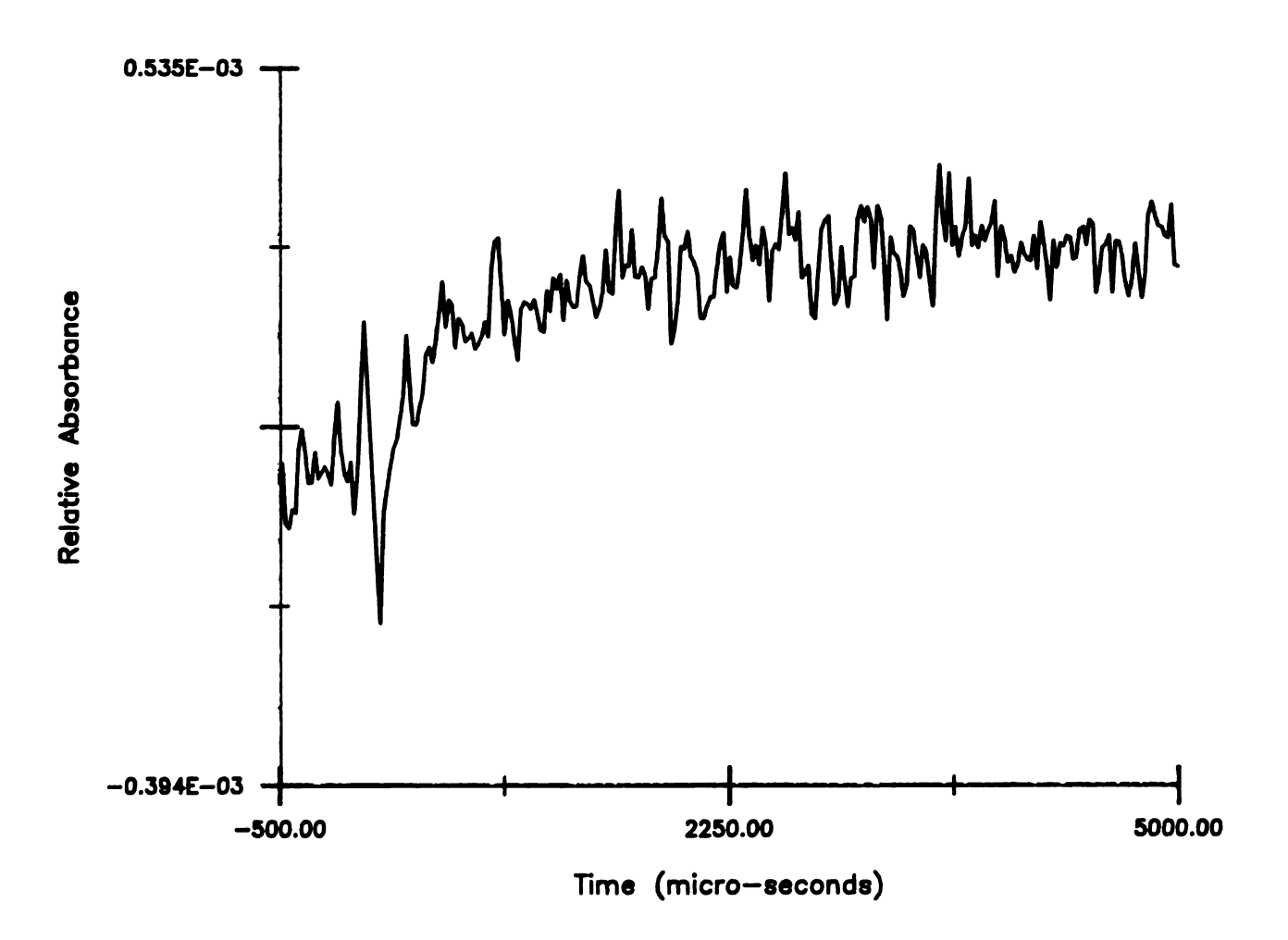
4.1.4 Neutral Red Absorbance Changes -

Operation of photochemistry pumps protons to the interior of the thylakoids in the oxidation of the PQ pool. Protons are also released to the interior by water oxidation. These protons are used by the ATPase in the production of ATP (see Figure 1.3). Studies performed in which Cresol Red, a non-permeant indicator dye, was used to show that external proton release and uptake can be time resolved (milliseconds or more; for a detailed discussion, see Junge (2)). Neutral Red (NR), a membrane permeable indicator dye, can respond to both external and internal proton release or uptake. Selective buffering of the external media by BSA will allow only the response of NR to internal proton release or uptake to be observed.

Figure 4.6 reveals the response of NR at 529 mm. Proton release is indicated by the increase in absorbance. The time scale of 40 ms is too short to show the eventual leveling off and decay in absorbance (0.5-1.0s). Two measurements were performed to obtain the trace. A standard sample with no NR present was run in which 25 flashes spaced 10 seconds apart were averaged. A second experiment was carried out under the same conditions with 40 $\mu \underline{M}$ NR. The former was then subtracted from the latter to obtain the trace in Figure 4.6.

Correlating the NR response to particular phenomena, such as the S_n state transition(s) responsible for proton release, has led to conflicting ideas as discussed in Chapter One. Experimentally, the controls Auslander and Junge established (22) are adequate. However, the integrity of the chloroplasts used and the reproducibility of their condition are suspect. It has been demonstrated that freshly prepared

NEUTRAL RED ABSORBANCE CHANGES. As discussed in the text, this is the result of subtracting the absorption changes at 529nm with 40 $\mu \underline{M}$ N.R. with those obtained without N.R. in solution. Both original data sets contained sharp negative peaks at time zero, subtraction took most of it out. Each data set also contained laser-induced scatter. Subtraction of one from another automatically eliminates the scatter.



chloroplasts, those stored at -40°C, and those under liquid nitrogen all show different proton release patterns as detected by NR. Freeze-thawed chloroplasts have membranes which are permeable to buffers such as HEPES, MES, and phosphate. Freshly prepared chloroplasts do not display this dependence on buffers. Both sets of chloroplasts continue to display otherwise normal photosynthetic activity.

These experiments show that in general the FAS is able to reproduce results in the literature concerning electrochromic band shifts, inhibitor effects, and proton release as measured by an indicator dye. The smallest significant absorbance change (see Figure 4.6) is 2.3 · 10⁻⁴ with a signal-to-noise per flash of 0.4. However there are experimentally some problems to resolve. Figures 4.5 and 4.6 reveal fast negative absorbance changes just after the laser flash. This is due principally to the failure of the cutoff filters to attenuate the laser line fully. Essentially, this introduces a "dead-time" of 100µs before useful information can be extracted. For sampling rates of up to 10µs per point (200kHz; 10ms for a full scan), subtraction of a separate data set containing only changes due to scattering gives reproducible results. Higher sampling rates (ranging from .06-2 µs per point or 16.6 - .5Mhz) are limited though.

A gating technique was tried which turns the PMT off for a few microseconds. (The method and equipment for this technique were developed by Buttner (75)). This entails making one of the first few dynodes in the dynode chain in the PMT highly negative with respect to the photocathode, thus preventing any electrons from leaving the photocathodic surface. During the duration of the gate pulse the laser

would be triggered, and, presumably, the PMT would be able to track after the gate was over the intensity changes as it would not have been affected by the laser flash. However, under continuous photon flux upon the photocathodic surface (from the probe beam), and while the gate is applied, electron carriers accumulate until the gate is is removed and a large electron flux then travels down the dynode chain. The immediate effect is an apparent large absorbance decrease upon turning the gate off lasting for hundreds of microseconds. While a laser scatter artifact is no longer observed the apparent absorbance decrease is of a larger magnitude and of a longer duration that attributed to the laser artifact.

As a result this technique is no longer pursued.

The laser scatter difficulty is being resolved through a redesign of the sample enclosure as mentioned in Chapter Two. Placement of the sample compartment closer to the PMT, restriction of the light path from the cell to the PMT window, choosing filters of higher attenuation at 640nm and lower attenuation at lower wavelengths, and ttenuation of the laser beam itself should remove the laser scatter. An increase in the signal-to-noise ratio is being affected by a redesign of the sample cell itself. The cell pathlength is begin decreased to 2.0mm from 5.0mm, and all the surfaces not directly involved or needed in the transmission of either the probe or excitation beams will be black-masked to reduce scattered light.

The above has already been partially completed, and the tests appear promising. The primary purpose of this project, the construction of a FAS, has been achieved and experiments of interest are being

devised. The modularity of the FAS is a tremendous advantage over commercial designs. Instrument modifications will be relatively simple, requiring only for the affected module to be replaced and/or modified. The computer interface is quite flexible, and literally requires only a change of software to accommodate differing experimental requirements.

4.2 PLANNED EXPERIMENTS

4.2.1 Spectral and Kinetic Identification of Z -

In the literature today there is evident much interest in the primary electron donor to P680. Since 1976 there has been inferred a relationship between Signals II, and II, and Z (49,50) has been inferred. Bocques-Bocquet (9), to explain the nano- and micro-second reduction times of P680⁺, has invoked the idea of two donors acting in Renger, using controversial "inside-out" TRIS-washed parallel. chloroplasts (52) and bromo-cresol purple, a non-permeant indicator dye, quantified proton release thought to be related to the redox reactions of Z and correlated it to the extent of P680 oxidation. O'Malley (11), has suggested that Z is a quinone, and in its oxidized state is a cation radical, Z.+, giving rise to an ESR detectable signal. Model studies he has performed on quinone cation radicals generated in 12 N H2 SO4 give remarkably similar ESR lineshapes to that of Signal II. Diner, at the 6th International Photosynthetic Congress, provided evidence of an optically detectable signal around 320nm seemingly correlated to P680⁺ reduction.

Other closely related components of PSII are also yielding information. The amino acid sequence of the P680 containing protein has apparently been determined by Trebst (19). Empirical models determining protein folding, regions of hydrophobicity, and hydrophilicity support general configurational models such as Johnson's et al. (62) for the OEC complex and its interactions with Z and P680.

Dekker et al. (76) have apparently obtained optically the difference spectrum of $Z^{*}-Z$, and kinetic data related to the reduction of Z^{*} in the UV region. Use of either a deuterium lamp or a zenon arc lamp should permit us to do likewise. An important set of experiments will be the correlation of the behaviour Signal II with that of Z.

Another set of studies will place emphasis on the extraction/reconstitution of Z. This is important because while a structure for Z has been proposed this can only serve as an unproved model until the component can be isolated and identified. Modification of ring substituents in Z-analogues, assuming Z is a quinone species, should yield much information regarding the requirements for electron transfer from the OEC through Z and into P680.

APPENDIX A

INTERACTIVE KINETIC OPERATING SYSTEM

VERSION 17-JUN-83
Dwight H. Lillie
Babcock Research Laboratory
Dept. of Chemistry
Michigan State University

[This is the interactive and initialization routine for the [AIM-65 microcomputer. The total operating system enables [the AIM-65 to perform very fast timing sequences or to upload [data from a NICOLET-1072 into the PDP-11.

[This version, as all previous versions, suffer from a lack of [raw memory in the AIM-65. Thus code is condensed as much as [possible, and this special documentation convention adopted for [use with HALCDC.

[There are two main assembly language subroutines which control the actual performance of the above functions. Linkage to these [routines currently is implemented through peeking at pre-defined [high locations in memory. For current implementation I've located [the pointers as such:

TIMING SUBROUTINE : \$FFC, \$FFD (10w/high byte)

(4092,4093)

NICOLET DUMP SUBR : \$FFA, \$FFB (10w/high byte)

(4090,4091)

This implementation has some advantages - namely in that fewer changes need to be made throughout the BASIC and ASSEMBLER code when modifications are (will be) made. At a later date when the AIM-65 is expanded to 64K these pointers will be relocated - preferably to zero-page; however, as BASIC keeps a number of pointers there - probably just under the SYSTEM routines.

```
[
          dimension the arrays to SI = 24 (for 4k of RAM)
1 SI = 24
3 DIM DE(SI), NA$(SI), AD(SI)
          define a function which will yield the floating point
          number of the addition of two bytes. These are useful for
[
          determing the address of a location store in two bytes in
          memory.
          ADDR is address of the low byte and ADDR+! is address of the
          high byte:
         FNFP(ADDR)=INT(PREK(ADDR))+INT(PREK(ADDR+1)*256)
        FNFP(I)=INT(PREK(I))+INT(PREK(I+1)+256)
5 DEF
7 TI$=" ":POKE 40962,16
[ find out what user wants to do
8 KK=0:GOSUB 800
10 PRINT"INPUT FUNCTION :: ":PRINT" ","1 - TIMING...REPEAT"
20 PRINT" ","2 - TIMING...NEW":PRINT" ","3 - DUMPING"
30 PRINT" ","4 - EXIT": INPUT J
40 IF J=4 THEN STOP
50 IF J=3THEN1000
60 IFJ=1ANDKK=1THEN385
          if j=2 then we just naturally fall through to the correct
          spot or if j=1 and we've never been here before - as
          indicated by kk
 this section devoted to setting up parameters for
[ performing a timing sequence
                        base for timing arrays in memory
          ND
                        number of device pulses per cycle
[ also initialize pointer to start of actual routine
     [
100
         KK=0:J=1:BA=FNFP(4092)
[ initialize entire array
120
        FOR I=OTO100:POKE BA+I,0:IF PEEK(BA+I)<>OTHEN9000:NEXT
prompt to get the necessary input
```

```
in order to set up a timing situation
           PRINT:PRINT:INPUT"TITLE : ";TI$
160
180
           INPUT"PULSES PER CYCLE: ":ND
190
           INPUT" OF ITERATIONS: ":NI
200
           K=BA+(ND-1)
210
           FOR I=0 TO ND-1
                         "; I+1 :PRINT
220
           PRINT"PULSE
           INPUT'NAME, DELAY, PIN: ": NAS (I+1), DE (I+1), AD (I+1)
230
           IF AD(I+1)=8 THEN AD(I+1)=12
260
270
           J=1:GOSUB 650
[ parameters are stored in arrays:
       <overflow byte for time><address><lsb of time><msb of time>
[ the offset between the arrays is the dimension of the arrays
[ last pulse to be sent is stored in the "bottom" and the first
  pulse is found ND+base+offset into initial byte of entire
[ allocation
280
           POKE K.OB:POKE K+SI*2.LB:POKE K+SI*3.HB:POKE K+SI.AD(I+1)
[ test to see if values are really there
           IF PEEK(K)<>OB OR PEEK(K+SI+3)<>HB THEN 9010
310
320
           IF PERK(K+SI+2) <> LB OR PERK(K+SI) <> AD(I+1) THEN 9010
330
           PRINT:PRINT:K=K-1
340
           NEXT
350
           J=0 :GOSUB 650
[ put the number of iterations in (HB+1,LB), and the number
[ of iterations (ND).
[ These live at the fixed offset of the BASE of device array
[ + size (SI) of array*4 + 1 - if number of devices
                          + 2 - if number of iterations
360
           POKE BA+SI*4+2,(HB+1):POKE BA+SI*4+3,LB:POKE BA+SI*4,ND
[ clear the screen and print the current timing setup
[ and then query for "go-ahead"
385
           GOSUB 800
390
           PRINT"...INITIALIZATION COMPLETED..."
420
           PRINT : PRINT
           PRINT"TITLE : ":TI$
430
440
           PRINT :PRINT"DEVICES : ";ND
           PRINT :PRINT "ITERATIONS : ":NI
450
460
           PRINT :PRINT"NAME",,"DELAY","ADDRESS"
470
           PRINT
           FOR I=1 TO ND:PRINT NA$(I),,,DE(I),AD(I):NEXT:PRINT:PRINT
480
520
           IF KK<>0 THEN 550
```

30	INPUT"READY(Y=1/N=0) "; J:IF J=0 THEN 385
	at the starting point and poke them into the routine and then go for it
50 60	POKE 4, PREK(4094): POKE5, PREK(4095): I=USR(0): POKE40962, 16 GOSUB 800: PRINT"EXPERIMENT COMPLETED": KK=1: GOTO10
	this routine returns the ***real*** time input as three bytes and which are then poked into the proper places for the timing code to find
50 70 90 00 20 40	TE=NI:IF J>0 THEN TE=DE(I+1) OB=INT(TE/65536):HB=INT((TE-OB*65536)/256) LB=INT(TE-OB*65536-HB*256):IF J=0 THEN 740 IF HB>0 OR LB=>150 THEN 740:LB=150 PRINT"MIN. LB DELAY TIME ADJUSTED TO 150" RETURN
	this routine will clear the terminal screen (HEATH ESCAPE CHARACTERS!) and return the cursor to the top left of the screen
300	PRINTCHR\$(27); CHR\$(72); CHR\$(27); CHR\$(74): RETURN
*******	NICOLET READOUT
	this section just calls the NICOLET UPLOADER. We peek into previously defined areas of memory to get the jump location and poke them into the USR jump handler.
	NOTE: sometimes the NICOLET fails to initialize itself properly at the start - if so, it can be forced into initialization by poking a value in.
.000 .010 .030 .040	INPUT"1 - GO AHEAD/O -RETURN : "; J:IF J=0 THEN 10 POKE4, PEEK (4090): POKE5, PEEK (4091): POKE 40962, 16 IFPEEK (40960) <> 1750RPEEK (40960) <> 191THENPOKE40960, 191: I=USR(0) GOTO1000
	ERROR MESSAGES - few as they are
•	this primarily seems to be a waste of memory space;

[however,	it	does	insure	that	timing	parameters	are	CORRECT!
	********		REFE			SEEREKE:	FERESESSES		
[
9000	PRINT"ARI	RAY	INIT	IALIZAT:	ION F	AILURE"	:STOP		
9010	PR INT"VAI	RIAB	LE T	EST FAII	LURE"	STOP			

```
TIMING CONTROL
  VERSION: 6.17.83
[ This routine directs a simple timing algorithm for use
[ with the specific hardware built for the AIM-65 micro-
[ computer. This routine is called from a BASIC controller
[ and is already initialized and parametically set up by
  HOOKUP:
          memory locations: FFE-FFF(16) - LB/HB OF where BASIC
                                              routine has to jump to
                                              start
                               FFC-FFD(16) - where assembly begins
                                                   Dwight H. Lillie
                                                   17-JUN-83
                                                   Babcock Research Lab
                                                   Dept. of Chemistry
                                                   Michigan State Univ.
*=3280
ASEMBL
SIZE
          =24
allocate size of blocks - 24 bytes each
           specify where assembled code starts
OBASE
           +=+SIZE
           *=*+SIZE
DBASE
           *=*+SIZE
TLBASE
THBASE
           *=*+SIZE
NUMBER
           *=*+1
INOT
           *=+1
           *=++2
ITERAT
TEMP1
           *=++2
           =$A001
DECODE
DDRA
           =$A003
TLATCH
           =$A004
ACR
           =$A00B
PCR
          -$A00C
IER
          =$A00E
IRQV
          =$A400
                                  real code begins here...as you
ſ
                                  can see - not too impressive
```

```
[
           for the time being disable possiblity of being interupted
[
           initialize the VIA
[
           store the address of the interupt service routine
[
              to the interupt handler J IRQV
[
           define porta as being all output
[
           set up the auxiliary control register -- ACR
[
           load a dummy time into the timer (T1) just to get things
[
              started
[
           define the type of interupts allowed
           and enable the interupts
START
  SEI
            $00
  LDA
   STA
           PCR
   STA
           INOT
   TAX
  TAY
  CLD
I
                                    load the interupt vector and store
                                    to handler
  LDA
            (ISR
  STA
           IRQV
  LDA
            >ISR
  STA
           IRQV+1
I
                                    get the
                                              of iterations as passed from
[
                                    the program and store in a
ſ
                                    temporary counter
  LDA
           ITERAT+1
   STA
           TEMP1+1
  LDA
           ITERAT
  STA
           TEMP1
   LDA
           $11111111
   STA
           DDRA
  STA
           DDRA-1
   LDA
           $11000000
   STA
           ACR
[
                                    to get things going give the timer a
dummy time to count through with all
[
                                    address lines deselected. This gives
[
                                    us a chance to get our act together
                                    and find ourselfs.
            SFF
   LDA
   STA
           TLATCH
   STA
           TLATCH+1
   LDA
            500111111
I
                                    enable interupts only from timer 1
   STA
           IER
  LDA
            $11000000
   STA
           IER
[
                                    enable processor to be interrupted
```

```
CLI
BEGLP
   LDX
           NUMBER
ITER
           LDA
                    DBASE-1,X
           DECODE
   STA
   I.DA
           TLBASE-1,X
   STA
           TLATCH+2
   LDA
           THBASE-1,X
   STA
           TLATCH+3
                    INOT
CHECK
           LDA
   BEQ
            CHECK
   DEC
           INOT
   LDY
           OBASE-1,X
   BEQ
            CONT
   LDA
            $FF
   STA
           TLBASE-1,X
   STA
           THBASE-1,X
VAIT
           LDA
                    INOT
           VAIT
   BEQ
   DEC
           INOT
   DEY
   BNE
           VAIT
           DEX
CONT
           ITER
   BNE
   DEC
           TEMP1+1
   BNE
           BEGLP
           ITERAT+1
   LDA
   STA
           TEMP1+1
   DEC
           TEMP1
   BNE
           BEGLP
PUAL
   LDA
           INOT
   BEQ
           PUAL
   SEI
   LDA
            $00
   STA
           INOT
   STA
           ACR
   STA
           TLATCH
   STA
           TLATCH+1
   STA
           TLATCH+2
   STA
           TLATCH+3
   RTS
ISR
                            deselect all possible address lines for now
            $FF
   LDA
   STA
           DECODE
[
                            set interupt flag to let world know
   LDA
            $01
   STA
            INOT
clear interupt flag by reading low latch of
                                timer
           TLATCH
   LDA
[
                            and go home
```

```
[
                 NICOLET READOUT
[ This subroutine is initiated from BASIC and directly handles
[ the data uploading from the NICOLET 1074 to the PDP-11. This
[ subroutine represents a reduction from 15 minutes for a 4K
[ memory dump to only about 3 to 4.
 SYSTEM SUBROUTINES:
                 OUTITY: BEA8(16) -- handles the actual output
                                        to the terminal
                                        requires character to be
                                        sent to be in the Acc.
  HOOKUP:
         memory locations: FF8-FF9(16) - LB/HB of where assembly
                                              begins
                              FFA-FFB(16) - LB/HB of where BASIC jumps
                                          to for beginning.
  MODIFICATIONS:
          23-ADG-83
          included a "termination" sequence at the conclusion of a
         nicolet dump. This aborts any "GET" in progress, and has
         no effect if one is not. Designed to work with HALCDC
  current memory requirments:
         276 bytes (23-aug-83)
                                              27-JUN-83
                                              Dwight H. Lillie
                                              Babcock Research Lab
                                              Dept. of Chemistry
                                              Michigan State Univ.
                 initialization _declaration
*=3000
ASEMBL
                 character storage from nicolet
.BYTE '.'
PERIOD
CR .BYTE J15
LF .BYTE J12
INOT
         *=*+1
DFLAG
         *=+1
```

```
.BYTE '-'
MINUS
PLUS
            BYTE '+'
ſ
[
                    encode the message in reverse to make it
ſ
                    easier to print
[
            .BYTE J12, J15, 'R', J12, J15, J12, J15
TERM
   .BYTE 'G', J12, J15, '{'
                    system allocations
           = $A000
PORTB
OUTTTY
           = SERAS
CRLF
           = $E9F0
ſ
                    this is where BASIC must jump for successful
[
                    transfer of control
ſ
START
            $00
   LDA
   STA
           DFLAG
                    define portB as all input except for bit 5
            $00010000
   LDA
   STA
           PORTB+2
CLEAR
   LDX
            $07
   LDA
            $00
LOOP
           DIGIT-1.X
   STA
   DEX
   BNE
           LOOP
SIGN
            $FF
   LDX
[
[
                    initially - let's give the "print" sign a bit of
[
                    time to go high before returning to BASIC
REGST
   LDA
           PORTB
   AND
            %10000000
   BNE
           PC1W
   DEX
   BNE
           REGST
I
                    if not high after 255 micro - go home
   JMP
           DONE
                    now wait for PC1 to go high
PC1W
           PORTB
   LDA
   AND
            500100000
   BEQ
           PC1V
[
well, it's time to start getting real data in
ĺ
                    now - read the sign first--
ſ
   LDA
           PORTB
```

```
$FF
   EOR
            500001111
   AND
   CMP
            $01
ſ
                    if not a minus then go on and test to make sure
   BNE
           NEXT
   LDA
           MINUS
   STA
           DIGIT
   JMP
           BFETCH
NEXT
            $00
   CMP
   BEQ
           CONT1
   LDA
            $01
CONT1
           PLUS
   LDA
   STA
           DIGIT
BFETCH
                   time to get rest of character - update pointer
            $01
   LDX
[
ſ
                   so...send a fetch, wait, and then read character
FETCH
   JSR
           SENDH
           TIAV
   JSR
   LDA
           PORTB
[
                   remember - the NICOLET has inverted logic so invert
[
                   the bits
   EOR
            $FF
and as the character is BCD mask off top 4
   AND
            %00001111
[
                   and convert to an ASCII character for presentation
   ORA
            %00110000
   STA
           DIGIT, X
   JSR
           CKPB7
[
                   and prepare to send another fetch
   JSR
           SENDL
   INX
ſ
                    in case our internal count is not accurate or we're
[
                   not synchronous with the NICOLET - we monitor whether
ſ
                   the NICOLET is telling us that's all the characters
[
                   for that number
   LDA
           INOT
   BNE
           OUTLP
[
                   reached end of the buffer for character yet?
            $07
   CPX
   BNE
           FETCH
[
                   if so then send a fetch so that NICOLET has time
                   to finish decoding the next character
                   and then print out the current character
OUTLP
           SENDH
   JSR
            $01
   LDX
```

```
I
                   number of characters put out is longer than that
                   read in as we have to send (cr><1f>
NCHAR
   LDA
           DIGIT-1,X
   JSR
           OUTTTY
   INX
            $0B
   CPI
   BCC
           NCHAR
                    if we're all done then re-inforce the earlier fetch
I
                   and go for a nice long wait
   JSR
           SENDH
   JSR
           LWAIT
   JMP
           SIGN
[
[
           DONE
[
                    it appears that we're all done dumping the data
[
                   so clean up and return back to (sigh) BASIC
[
DONE
            $01
   LDA
           DFLAG
   STA
I
[
                   send out a termination message to "CDC" and return
[
                   to interactive BASIC
[
   LDX
            11
DLP
           JSR
                   LWAIT
   LDA
           TERM-1,X
   JSR
           OUTTIY
   DEX
   BNE
           DLP
   RTS
[
[
           WAIT
[
                   do all of our waiting here.
ſ
                   recall that the AIN can run faster than the
                   NICOLET can!
[
[
LWAIT
            $FF
   LDY
BAGA
   DEY
   BNE
           BAGA
   RTS
[
                   on just a normal WAIT should be roughly 40-100
[
                   micro-seconds and that's probably long enough
   TIAV
   RTS
I
           SENDH _SENDL
                    this is for bit 5 of portB and tells the NICOLET
[
[
                   when we're doing another fetch
SENDH
```

```
LDA
           PORTB
   ORA
            %00010000
   STA
           PORTB
   RTS
SENDL
   LDA
           PORTB
   AND
            $11101111
   STA
           PORTB
   RTS
[
           CKPB7
I
                    check on the status of PB-7
[
                    the NICOLET doesn't seem to tend this well so make
[
                    sure it really is null before drawing any hasty
[
                    conclusions
[
CKPB7
           LDY
                     SOA
ONE
   DEY
  BEQ
           ENDCHR
   LDA
           PORTB
            %01000000
   AND
   BNE
           ONE
  LDA
            $00
   STA
           INOT
  RTS
ENDCHR
  LDA
            $01
   STA
           INOT
  RTS
[
                   now set up the already defined linkage for
[
                    the AIM-65.
  -$FF8
[
                    assembly begins here
, WORD
           ASEMBL
                   and the BASIC must jump to here
, WORD
           START
, END
```

LIST OF REFERENCES

LIST OF REFERENCES

- 1. Norrish and Porter (1949), Proc. Roy. Soc., Ser. A 200, 284-300.
- 2. Junge, W. (1976), Chemistry and Biochemistry of Plant Pigments Vol II Chapt 22, Goodwin, T.W., ed., Academic Press, NY.
- 3. Mathis (1977), <u>Primary Processes of Photosynthesis</u> 269-302, ed., Barber, J.
- 4. Van Best, J.A. and Mathis, P. (1979), Photochem. Photobio. 31, 89-92.
- 5. Van Best, J.A. and Mathis, P. (1978), Rev. Sci. Instr. 49 (9), 1332-1334.
- 6. Junge, W. (1981), Biochim. Biophys. Acta. 141-152.
- 7. Crofts, A. (1974), Biochim. Biophys. Acta. 357, 78-88.
- 8. Ingle, J.D., Crouch, S.R. (1971), <u>Anal.</u> <u>Chem.</u> 43, 1331-1334.
- 9. Bouges-Bocquet, B. (1980), <u>Biochim.</u> <u>Biophys.</u> <u>Acta.</u> 594, 85-103.
- 10. Bernstein, M., Rothberg, L.J., Peters, K.S. (1982), Chem. Phys. Lett. 91, 4, 315-319.
- 11. O'Malley, P. and Babcock, J., <u>Biochim. Biophys. Acta.</u> (submitted).

- 12. Bassham, J.A., and Calvin, M. (1957), <u>The Path of Carbon in Photosynthesis</u> 1-104, Prentice Hall, Englewood Cliffs, NJ.
- 13. Hill, R., and Bendall, F. (1960), Nature 1,86,136.
- 14. Hind, R., and Olson, J.M. (1968), Ann. Rev. Plant. Physiol. 19, 249.
- 15. Avron, M. (1975), <u>Bioenergetics of Photosynthesis</u> 374-387, Govindjee, R., ed., Academic Press, Inc, New York, NY.
- 16. Clayton, R.K. (1980), <u>Photosynthesis:</u> <u>Physical</u>
 <u>Mechanisms and Chemical Patterns</u> 88-228, Cambridge Univ.
 Press, New York, NY.
- 17. Ross, R.T. and Calvin, M. (1967), J. Biophys. 7, 595.
- 18. Van Best, J.A. and Mathis, P. (1978), <u>Biochim.</u> <u>Biophys.</u> <u>Acta.</u> 503, 178-188.
- 19. Trebst, A., private communication.
- 20. Jortner, J. (1980), <u>Biochim.</u> <u>Biophys.</u> <u>Acta.</u> 594, 193-230.
- 21. Haan, G.A., Duysens, L.N.N., and Egberts, D.J.N. (1974), Biochim. Biophys. Acta. 8, 409-421.
- 22. Auslander, W. and Junge, W. (1975), <u>FEBS Lett.</u> 59, 310-315.
- 23. Robinson, H.H., Sharp, R.R., Yocum, C.F. (1980), <u>Biochem.</u>
 <u>Biophys.</u> <u>Res.</u> <u>Commun.</u> 93, 755-761.
- 24. Sun, A.S.K., and Sauer, K., <u>Biochim</u>, <u>Biophys</u>, <u>Acta</u>, (1971), 234, 503-508.
- 25. Yerkes, C.T. (1979), M.S. Thesis, The Kinetics of

Electron Transport in Chloroplast Photosystem II 41-44.

- 26. Buttner, B., Ph.D. Thesis <u>Induced and Natural Delayed Luminescence of Green Plant Photosynthesis</u> in press, 31-32.
- 27. Govindjee, and Govindjee, R. (1975), <u>Bioenergetics of Photosynthesis</u> 1-150, ed., Govindjee, R., Academic Press, New York, NY.
- 28. Pearlstein, R.M. (1982), Photosynthesisu Vol I Energy Conversion by Plants and Bacteris 293-330, ed., Govindjee, R., Academic Press, New York, NY.
- 29. Ke, B. (1972), Arch. Biochem. Biophys. 152,70-77.
- 30. Norris, J.R., Uphaus, R.A., Crespi, H., and Katz, J.J., (1971), Proc. Nat'l. Acad. Sci. USA 68, 625-628.
- 31. Norris, J.R., Scheer, H., Druyan, M.E., and Katz, J.J., (1974), Proc. Nat'l. Acad. Sci. USA 71, 4897-4900.
- 32. Davis, M.S., Forman, A., and Fajer, J. (1979), Proc. Nat'l. Acad. Sci. USA 76, 4170-4174.
- 33. Wasielewski, M.R., Norris, J.R., Crespi, H.L., and Harper, J. (1981), <u>J. Am. Chem. Soc.</u> 103, 7664-7665.
- 34. Homan, P.H., (1973), Eur. J. Biochem. 33, 247-252.
- 35. Meites, L., The General Multiparametric Curve-Fitting <u>Program CFT4Aπ</u> (1976), Computing Laboratory, Dept. of Chemistry, Clarkson College of Technology, Potsdam, NY, publ.
- 36. Malkin, R., Beardon, J. (1975), <u>Biochim.</u> <u>Biophys.</u> <u>Acta.</u> 396, 250-259.
- 37. Stiehl, H.H., Witt, H.T. (1969), Z. Naturforsch. Teil B 24, 1588.

- 38. Haveman, J., Mathis, P. (1979), <u>Biochim</u>, <u>Biophys</u>, <u>Acta</u>, 440, 346-355.
- 39. Malkin, R., Bearden, A.J. (1975), <u>Biochim Biophy Acta.</u> 396, 250-259.
- 40. Dutton, P.L. (1967), Photochem. Photobio. 24, 655-667.
- 41. Babcock, G.T., and Sauer, K. (1975), <u>Biochim.</u> <u>Biophys.</u> <u>Acta.</u> 375, 315-328.
- 42. Joliet, P., Barbieri, G., and Chabaud, R. (1969), Photochem. Photobio. 10, 309-329.
- 43. Kok, B., Forbush, B., and McGloin, M. (1970), <u>Photochem.</u>
 <u>Photobio.</u> 11, 457-475.
- 44. Junge, W., Renger, G., and Auslander, W. (1979), <u>FEBS</u>
 <u>Lett.</u> 79, 155-159.
- 45. Renger, G. (1977), <u>FEBS</u> <u>Lett.</u> 81, 223-228.
- 46. Fowler, C.F. (1977), <u>Biochim. Biophys. Acts.</u> 462, 414-421.
- 47. Antonini, E., and Brunoni, M., Hemoglobin and Myoglobin and Their Reactions with Ligands (1971), North-Holland publ., Amsterdam.
- 48. Blankenship, R.E., Babcock, G.T., and Sauer, K. (1975), Biochim, Biophys. Acta. 387, 165-175.
- 49. Blankenship, R.E., Babcock, G.T., and Sauer, K. (1976), Biochim. Biophys. Acts. 396, 48-62.
- 50. Babcock, G.T., Blankenship, R.E., and Sauer, K. (1976), FEBS Lett. 61, 286-289.
- 51. Renger, G., and Weiss, W. (1976), FEBS Lett. 722, 1-11.

- 52. Renger, G., and Voelker, M. (1982), <u>FEBS Lett.</u> 149, 203-207.
- 53. Hong, Y.Q., Forster, V., and Junge, W (1981)., <u>FEBS Lett.</u> 132, 247-251.
- 54. Junge, W., and Witt, H.T. (1968), Z. Naturforsch. 236, 244.
- 55. Liptay, W. (1969), Anal. Chem. 81, 195.
- 56. Schliephake, W., Junge, W., and Witt, H.T. (1968), Z. Naturforsch 236, 1571.
- 57. Hong, Y.Q., and Junge, W. (1983), <u>Biochim.</u> <u>Biophys.</u> <u>Acta.</u> 722, 197-208.
- 58. Theg, S.M., and Junge, W. (1983), <u>Biochim</u>, <u>Biophys</u>, <u>Acta</u>, 723, 294-307.
- 59. Khanna, R., Wagner, R., Junge, W., and Govindjee (1980), FEBS Lett. 121, 222-224.
- 60. Velthuys, B.R. (1980), FEBS Lett. 115, 167-170.
- 61. Junge, W., Auslander, W., McGeer, A.J., and Runge, T. (1979), <u>Biochim.</u> <u>Biophys.</u> <u>Acta.</u> 546, 121-141.
- 62. Johnson, J.D., Pfister, V.R., Hohmann, P.H. (1983), Biochim. Biophys. Acta. 723, 256-265.
- 63. Holten, D., Hoganson, C., Windosr, M.W., Schenck, C.C., W.W., Migus, A., Fork, R.L., and Shank, C.V. (1980), Biochim. Biophys. Acta. 592, 461-477.
- 64. WITT, H.T. (1979), <u>Biochim</u>, <u>Biophys</u>, <u>Acta</u>, 505, 355-427.
- 65. Johnson, L., HALCDC, MAC c1979, public domain.

- 66. Dye, J.L., and Nicely, V.A. (1971), <u>J. Chem.</u> <u>Ed.</u> 48, 433.
- 67. Ghanotakis, D.F., and Buttner, W.J. (unpublished data).
- 68. Clayton, R.K. (1980), <u>Photosynthesis:</u> <u>Physical</u>
 <u>Mechanisms and Chemical Patterns</u> 205, Cambridge Univ.
 Press, New York, NY.
- 69. Reinwald, E., Stiehl, H.H., and Rumberg B. (1968), Z. Naturforsch 2365, 1616-1617.
- 70. Amesz, J., and De Grooth, B.G. (1976), <u>Biochim.</u> <u>Biophys.</u> <u>Acta.</u> 440, 301-313.
- 71. Schmidt, S., Reich, R., and Witt, H.T. (1969), Z. Naturforsch 246, 1428-1431.
- 72. RS-232C INTERFACE FOR AIM 65, Document R6500 NO8, Rev 1, July 1979, Rockwell Int'l Corp., Newport Beach, CA.
- 73. R6522 VERSATILE INTERFACE ADAPTER (VIA), Document 29000 D47, Order No D47, Rev 4, Nov. 1981, Rockwell Int'1 Corp., Newport Beach, CA.
- 74. Buttner, B., Ph.D. Thesis <u>Induced and Natural Delayed</u>
 <u>Luminescence of Green Plant Photosynthesis</u> (in press).
- 75. Dekker, J.P., van Gorkom, H.J., Brok, M., and Ouwehand, L., <u>Biochim.</u> <u>Biophys Acta.</u> (submitted).
- 76. Joliet, P., Delosme, R., and Joliet, A. (1977), <u>Biochim.</u>
 <u>Biophys.</u> <u>Acta</u> 459, 47-57.